

$[\chi(i|\mathbf{R})]_2^0$ are no longer equal, and in general both even and odd, zero wave-vector irreducible representations occur in the reduction (see for example the reduction of the symmetrized Kronecker squares of $\Delta^5, \Delta^3, X^1, \dots, X^4, W^1$, and W^2 in diamond as given by Birman⁵).

The fraction of wave vectors which lie on symmetry

lines or points in the Brillouin zone is of order $N^{-2/3}$, where N is the number of unit cells in the crystal sample. Thus the selection rule forbidding participation of overtone states in absorption which we have proved for phonons of general wave vector can, for all practical purposes, be assumed to apply to phonons of all wave vectors.

PHYSICAL REVIEW

VOLUME 137, NUMBER 6A

15 MARCH 1965

Theory of Stimulated Brillouin and Raman Scattering*

Y. R. SHEN† AND N. BLOEMBERGEN

Gordon McKay Laboratory, Harvard University, Cambridge, Massachusetts

(Received 19 October 1964)

Stimulated Raman and Brillouin scattering can be described as the interaction of several light waves with optical and acoustic-phonon waves, respectively. The coupling parameters can be derived both classically and quantum mechanically. A prototype solution is given for the coupling of infinite plane Stokes and anti-Stokes waves satisfying appropriate boundary conditions on a plane-parallel Raman cell, in which the laser intensity is assumed a constant parameter. Saturation effects, generation of higher order Raman radiation, and the effect of mode structure in the laser beam are treated in a more approximate and qualitative fashion. The theory can explain at least qualitatively most of the experimental findings, including the directional properties of the Raman radiation. Ideal experiments for clarifying the mechanism of the Raman effect are suggested.

I. INTRODUCTION

THE coherent part of the interaction between light and matter can be described by linear and nonlinear susceptibilities. The nuclear motion modifies the scattering of light by electrons. This leads to Raman and Brillouin scattered light with a characteristic frequency shift. Brillouin¹ studied the behavior of the interaction of light with acoustic waves. The Raman effect² can be described as the interaction of light with optical phonons. The spontaneous Raman scattering has long become an important tool for studying the vibronic structure of molecules and crystals.

Recently, Woodbury and Ng³ found accidentally that a ruby laser, Q switched with a nitrobenzene Kerr cell, emitted a strong radiation at 7670 Å, in addition to the normal ruby laser light at 6943 Å. It was soon recognized by Eckhardt *et al.*⁴ as the stimulated Stokes radiation from the nitrobenzene. When different liquids are inserted in the laser resonator, different frequencies are emitted. They are displaced from the ruby frequency by

an amount corresponding to a vibrational frequency of the liquids. In addition, the displaced radiation has the following characteristics. (1) Only the frequencies belonging to the sharpest and the most intense spontaneous Raman lines show up. (2) It has a definite threshold of excitation. (3) It is highly directional. (4) The linewidth is much narrower than that of the spontaneous line. (5) Higher order Stokes radiations occur at exact harmonics of the first vibrational transition. The stimulated Raman spectra of many liquids,^{4,5} solids,⁶ and gases⁷ have been reported. Terhune⁸ put the cell outside the laser resonator and was able to detect the anti-Stokes radiation emitted forward in a characteristic ring pattern. Higher order Stokes and anti-Stokes absorption and emission rings have also been observed.⁸⁻¹⁰ More recently, the detection of stimulated Brillouin scattering was reported by Chiao *et al.*¹¹

⁵ M. Geller, D. P. Bortfeld, and W. R. Sooy, *Appl. Phys. Letters* **3**, 36 (1963).

⁶ G. Eckhardt, D. P. Bortfeld, and M. Geller, *Appl. Phys. Letters* **3**, 137 (1963).

⁷ R. W. Minck, R. W. Terhune, and W. G. Rado, *Appl. Phys. Letters* **3**, 181 (1963).

⁸ R. W. Terhune, *Bull. Am. Phys. Soc.* **8**, 359 (1963); *Solid State Design* **4**, 38 (1963).

⁹ H. J. Zeiger and P. E. Tannenwald, *Proceedings of Third International Conference on Quantum Electronics, Paris, February 1963*, edited by P. Grivet and N. Bloembergen (Columbia University Press, New York, 1964), p. 1589.

¹⁰ R. Y. Chiao and B. P. Stoicheff, *Phys. Rev. Letters* **12**, 290 (1964).

¹¹ R. Y. Chiao, C. H. Townes, and B. P. Stoicheff, *Phys. Rev. Letters* **12**, 592 (1964).

* This research was supported jointly by the U. S. Office of Naval Research, the Signal Corps of the U. S. Army, the U. S. Air Force and the Advanced Research Projects Agency.

† Present address: Department of Physics, University of California, Berkeley, California.

¹ L. Brillouin, *Ann. Phys. (Paris)* **17**, 88 (1922).

² C. V. Raman, *Indian J. Phys.* **2**, 387 (1928); C. V. Raman and U. S. Krishnan, *Nature* **121**, 501 (1928).

³ E. J. Woodbury and W. K. Ng, *Proc. IRE* **50**, 2367 (1962).

⁴ G. Eckhardt, R. W. Hellwarth, F. J. McClung, S. E. Schwarz, D. Weiner, and E. J. Woodbury, *Phys. Rev. Letters* **9**, 455 (1962).

The theory of stimulated Raman effect has been discussed by many authors,^{9,12-19} both from the classical and from the quantum-mechanical points of view. The existence of a threshold for stimulated radiation is well explained. Although a qualitative explanation of many features has been given, there are still a number of important experimental observations²⁰ which have received no detailed explanation. In a recent communication,²¹ a description of the stimulated Raman effect was given in terms of a coupling between vibrational and light waves. The coupled wave approach in nonlinear optics was introduced by Armstrong *et al.*²²

In this paper a more detailed account of the coupled wave theory is presented. Nevertheless, it should be emphasized that a number of simplifying assumptions must be made in the theory, which thus far have not been met under the actual experimental conditions. In particular, the mode structure and nonuniformity of the laser beam are not in agreement with the assumption of uniform plane waves of infinite lateral extent. Depletion of the laser power implies that the laser field may not be treated as a fixed constant parameter. Transient effects may cause deviations from a steady-state description.

In Sec. II a classical discussion on the coupling of vibrational waves and light waves via a molecular system is given. If there are many photons in the radiation field it can properly be described by classical waves.^{23,24} The same is true for vibrational fields. In the treatment of coupled-wave problems, the classical description is even more appropriate since then the decay or amplification of the waves depends on the relative phases among them. If in the quantum description, the number of quanta is prescribed, the phases will be completely undetermined as required by the uncertainty principle. The quantum analog of the classical treatment is obtained from the so-called coherent states of the field, which have recently been investigated in much detail by Glauber.²⁴ In Sec. II, the equations of motion (or the wave equations) for the coupled-wave problem

are derived from the Lagrangian density. The coupling parameters are given by the properties of the medium. They can be derived from the classical model of Placzek²⁵ in the case of Raman scattering, and from the photoelastic coupling model in the case of Brillouin scattering. Except for the difference in vibrational frequencies and dispersion, the Brillouin scattering is formally identical to the Raman scattering. All the discussions on Raman scattering therefore apply to Brillouin scattering with only slight modification. Section III gives a quantum-mechanical derivation of the coupling parameters. A microscopic expression of the Raman susceptibility is obtained and compared with the classical expression. The coupled wave equations are solved in Secs. IV and V. It is shown how in the limit of high damping on the vibrational waves, the solution leads to the stimulated Raman emission. In principle, the amplification of the Stokes waves is very similar to that of a parametric-down converter. If one of the two low-frequency component waves is highly damped, the other will be amplified. The solution of the coupled Stokes and anti-Stokes wave equations shows that there can be no amplification for either wave in the direction of linear momentum matching condition. The Stokes and anti-Stokes waves are coupled most strongly near the momentum matching direction. In other directions, they are also coupled, although rather weakly. In consequence, for each Stokes wave generated or amplified in the medium, there is always a corresponding anti-Stokes wave dragging along. The angular distribution of the anti-Stokes intensity shows a maximum at a slightly greater angle than the exact phase-matched direction. As the interaction length is increased, the laser power will eventually be depleted, and the Stokes and anti-Stokes intensity will level off to their maxima. The Stokes and anti-Stokes radiation can, in turn, become a pump source to generate second-order Raman radiation and so on. This saturation effect is discussed in Sec. VI. The total laser power is not completely depleted only because the beam is multimoded, nonhomogeneous, and finite in cross section. In the real experiments, the multimode structure of the laser beam makes the problem very complex. Waves in different modes may interact to generate new frequencies parametrically. These parametric processes are responsible for the experimental observation of Stokes and anti-Stokes rings of many orders. The generation of higher order radiation and the effect of the multimode structure are discussed in Secs. VII and VIII. Owing to the complexity of the problem, only a qualitative discussion is given. Because of the close coupling of many modes, the Raman signal will show fluctuations and will depend in a sensitive way on the detailed geometry. In Sec. IX the theoretical results are shown to be in qualitative, or sometimes quantitative, agreement with the experimental results. New

¹² R. W. Hellwarth, *Phys. Rev.* **130**, 1850 (1963).

¹³ N. Bloembergen, *Proceedings of the Third International Conference on Quantum Electronics, Paris, February 1963*, edited by P. Grivet and N. Bloembergen (Columbia University Press, New York, 1964), p. 1501.

¹⁴ R. Loudon, *Proc. Phys. Soc. (London)* **A82**, 393 (1963); *Proc. Roy. Soc. (London)* **A275**, 218 (1963).

¹⁵ R. W. Terhune, *Solid State Design* **4**, 38 (1963).

¹⁶ E. Garmino, F. Pandarese, and C. H. Townes, *Phys. Rev. Letters* **11**, 160 (1963).

¹⁷ A. Javan, *Rendiconti Scuola Internazionale Enrico Fermi, Corso 22, August 1963* (Academic Press Inc., New York, 1965).

¹⁸ R. W. Hellwarth, *Appl. Opt.* **2**, 847 (1963); R. W. Hellwarth, *Current Sci. India* **33**, 129 (1964).

¹⁹ H. J. Zeiger, P. E. Tannenwald, S. Kern, and R. Herendeen, *Phys. Rev. Letters* **11**, 419 (1963).

²⁰ See, for example, B. P. Stoicheff, *Phys. Letters* **7**, 186 (1963).

²¹ N. Bloembergen and Y. R. Shen, *Phys. Rev. Letters* **12**, 504 (1964).

²² J. A. Armstrong, N. Bloembergen, J. Ducuing, and P. Pershan, *Phys. Rev.* **127**, 1918 (1962).

²³ E. T. Jaynes and F. W. Cummings, *IEEE* **51**, 89 (1963).

²⁴ R. Glauber, *Phys. Rev.* **130**, 2529 (1963); **131**, 2766 (1963).

²⁵ G. Placzek, *Max Handbuch der Radiologie*, edited by E. Marx (Academische Verlagsgesellschaft, Leipzig, Germany, 1934), 2nd ed., Vol. VI, Part II, p. 209-374.

experiments are however suggested to test the details of the theory.

II. THE CLASSICAL DESCRIPTION

The wave equations can be derived from the Lagrangian density of the system. Let us assume a dilute, isotropic medium. The Lagrangian density is given by

$$L = L_{\text{rad}} + L_{\text{vib}} + L_{\text{int}}, \quad (1)$$

where $L_{\text{rad}} = \frac{1}{2}(E^2 - B^2)$, assuming transverse waves. For the Raman effect, optical phonon waves are involved. We have

$$\begin{aligned} L_{\text{vib}} &= \frac{1}{2}\dot{Q}_v^2 - \frac{1}{2}\omega_0^2 Q_v^2 + \frac{1}{2}\beta(\nabla Q_v)^2, \\ L_{\text{int}} &= N\alpha\mathbf{E}\mathbf{E}. \end{aligned} \quad (2)$$

Here $\mathbf{Q}_v = \mathbf{R}(2\rho)^{1/2}$ is the normal coordinate, \mathbf{R} is the relative displacement of the nuclear positions, ρ is the reduced mass density, and α is the optical polarizability tensor of the molecule. In the Placzek model,²⁵ α is written as a linear function of \mathbf{Q}_v .

$$\alpha = \alpha_0 + (\partial\alpha/\partial Q_v)_0 \mathbf{Q}_v \quad (3)$$

or in tensorial notation, $\alpha^{ij} = \alpha_0^{ij} + (\partial\alpha^{ij}/\partial Q_v^k)_0 Q_v^k$. If this is inserted into L_{int} , one obtains a coupling energy between light and vibrational waves proportional to $\mathbf{Q}_v\mathbf{E}\mathbf{E}$. The equation of motion for the vibrational wave is now obtained from variations of L ,

$$\ddot{Q}_v^k + \beta\nabla^2 Q_v^k + \omega_0^2 Q_v^k + 2\Gamma\dot{Q}_v^k = N(\partial\alpha^{ij}/\partial Q_v^k)_0 E^i E^j. \quad (4)$$

The damping term $2\Gamma\dot{Q}_v$ is added phenomenologically. For $\mathbf{Q}_v \sim \exp(i\mathbf{k}_v \cdot \mathbf{r})$, the natural frequency of vibration is $\omega_v^0 = [\omega_0^2 - \beta k_v^2]^{1/2}$. The damping constant Γ is then clearly a function of k_v . Note that the wave has a negative dispersion for $\beta > 0$.

Assume the presence of only four waves, the vibrational wave at ω_v and light waves at ω_l , ω_s , and ω_a with $\omega_a - \omega_l = \omega_l - \omega_s = \omega_v$. For $\mathbf{Q}_v \sim e^{-i\omega_v t}$, we have

$$\begin{aligned} \beta\nabla^2 \mathbf{Q}_v + (\omega_0^2 - \omega_v^2)\mathbf{Q}_v - i2\omega_v\Gamma\dot{\mathbf{Q}}_v \\ = N(\partial\alpha/\partial Q)_0: [\mathbf{E}_l \mathbf{E}_s^* + \mathbf{E}_a \mathbf{E}_l^*]. \end{aligned} \quad (5)$$

The wave equations for \mathbf{E}_s , \mathbf{E}_a , and \mathbf{E}_l are

$$\begin{aligned} \nabla \times (\nabla \times \mathbf{E}_s) - (\epsilon_s \omega_s^2 / c^2) \mathbf{E}_s \\ = (4\pi \omega_s^2 / c^2) N(\partial\alpha/\partial Q)_0: \mathbf{Q}_v^* \mathbf{E}_l, \end{aligned} \quad (6a)$$

$$\begin{aligned} \nabla \times (\nabla \times \mathbf{E}_a) - (\epsilon_a \omega_a^2 / c^2) \mathbf{E}_a \\ = (4\pi \omega_a^2 / c^2) N(\partial\alpha/\partial Q)_0: \mathbf{Q}_v \mathbf{E}_l, \end{aligned} \quad (6b)$$

$$\begin{aligned} \nabla \times (\nabla \times \mathbf{E}_l) - (\epsilon_l \omega_l^2 / c^2) \mathbf{E}_l \\ = (4\pi \omega_l^2 / c^2) N(\partial\alpha/\partial Q)_0: [\mathbf{Q}_v \mathbf{E}_s + \mathbf{Q}_v^* \mathbf{E}_a]. \end{aligned} \quad (6c)$$

Assume further that the depletion of laser power is negligible, so that the amplitude of \mathbf{E}_l is a constant parameter in the equations. The saturation effect due to depletion of laser power will be considered in Sec. VI. Assume furthermore that \mathbf{E}_a is absent. These simplifying conditions will illustrate the generation of stimulated Stokes radiation. The complete solution of coupled Stokes and anti-Stokes generation will be given in

Sec. V. The remaining Eqs. (5) and (6a) can now be solved simultaneously. The solutions have the form $\mathbf{E}_s \sim \exp[i(\mathbf{k}_s \cdot \mathbf{r} - \omega_s t)]$ and $\mathbf{Q}_v \sim \exp[i(\mathbf{k}_v \cdot \mathbf{r} - \omega_v t)]$ with $\mathbf{E}_l = \mathbf{E}_l \exp[i(\mathbf{k}_l \cdot \mathbf{r} - \omega_l t)]$ and $\mathbf{k}_l = \mathbf{k}_s + \mathbf{k}_v$. From Eq. (5), we find

$$\mathbf{Q}_v = -N(\partial\alpha/\partial Q)_0: \mathbf{E}_l \mathbf{E}_s^* / (\omega_v^2 - \omega_0^2 + \beta k_v^2 + i2\omega_v\Gamma).$$

If the nonlinear coupling is small, then the wave vectors can be obtained, in the first approximation, from the linear matching condition $\mathbf{k}_l = \mathbf{k}_s^0 + \mathbf{k}_v^0$, the change due to nonlinear coupling being neglected. This approximation can be justified in the case of highly damped vibrational waves as will be discussed in detail in Sec. IV. Substitution of the expression of \mathbf{Q}_v into Eq. (6a) leads to

$$\nabla \times (\nabla \times \mathbf{E}_s) - (\omega_s^2 / c^2) [\epsilon_s + 4\pi \chi_R \mathbf{E}_l \mathbf{E}_l^*] \mathbf{E}_s = 0, \quad (7)$$

where the fourth-rank Raman susceptibility is defined as

$$\chi_R^{ijmn} = -N \sum_k (\partial\alpha^{ij}/\partial Q_v^k)_0 (\partial\alpha^{mn}/\partial Q_v^k)_0 / D^*,$$

with

$$\begin{aligned} D^* &= \omega_v^2 - \omega_0^2 - i2\omega_v\Gamma, \\ \omega_v^0 &= \omega_0^2 - \beta k_v^2. \end{aligned}$$

In this paper, the field intensity and the polarization are defined as²⁶

$$\begin{aligned} \mathbf{E}_i(t) &= \text{Re}(\mathbf{E}_i + \mathbf{E}_i^*) = \text{Re}\{\mathbf{E}_i(\omega_i) \exp(-i\omega_i t) \\ &\quad + \mathbf{E}_i(-\omega_i) \exp(i\omega_i t)\}, \\ \mathbf{P}_i(t) &= \text{Re}(\mathbf{P}_i + \mathbf{P}_i^*) = \text{Re}\{\mathbf{P}_i(\omega_i) \exp(-i\omega_i t) \\ &\quad + \mathbf{P}_i(-\omega_i) \exp(i\omega_i t)\}. \end{aligned} \quad (8)$$

The real part of χ_R changes the index of refraction at ω_s , whereas the imaginary part, being negative, leads to amplification at ω_s .

Similar arguments can be applied to the Brillouin effect, where acoustic waves are involved. The Lagrangian density has the terms,

$$\begin{aligned} L_{\text{vib}} &= \frac{1}{2}\rho_a \dot{A}^2 - \frac{1}{2}C_a (\nabla A)^2, \\ L_{\text{int}} &= \mathbf{p}(\nabla A)\mathbf{E}\mathbf{E}, \end{aligned} \quad (9)$$

where A is the displacement of nuclei, C_a is the linear elastic modulus, \mathbf{p} is the photoelastic tensor of the order of unity, and ρ_a is the mass density. The equation of motion for the acoustic wave is

$$\rho_a \ddot{A} - C_a \nabla^2 A + 2\Gamma\rho_a \dot{A} = \mathbf{p}\nabla(\mathbf{E}\mathbf{E}). \quad (10)$$

A particular steady-state solution is again obtained by treating E_l as a fixed parameter and considering only two wave equations for the acoustic vibrational wave at ω_a and the Brillouin shifted light wave at ω_b with $\omega_l - \omega_b = \omega_a$

$$\begin{aligned} C_a \nabla^2 A + \omega_a^2 \rho_a A + i2\omega_a \Gamma \rho_a \dot{A} &= -\mathbf{p}\nabla(E_l E_b^*), \\ \nabla \times (\nabla \times \mathbf{E}_b) - (\omega_b^2 \epsilon_b / c^2) \mathbf{E}_b &= (4\pi \omega_b^2 / c^2) \mathbf{p} E_l \nabla A^*. \end{aligned} \quad (11)$$

²⁶ P. S. Pershan, *Progress in Optics*, edited by E. Wolf (North-Holland Publishing Company, Amsterdam, 1964).

With the linear approximation on the wave vector \mathbf{k}_a , we find

$$\nabla \times (\nabla \times \mathbf{E}_b) - (\omega_b^2/c^2) [\boldsymbol{\epsilon}_b + 4\pi\boldsymbol{\kappa}_B \mathbf{E}_l \mathbf{E}_l^*] \mathbf{E}_b = 0,$$

where the fourth-rank Brillouin susceptibility tensor is

$$\chi_B^{ijmn} = \sum_k p^{ijk} p^{mkn} k_v^2 / \rho_a (\omega_a^2 - \omega_a^0{}^2 - i2\omega_a \Gamma), \quad (12)$$

$$\omega_a^0{}^2 = k_a^0{}^2 C_a / \rho_a.$$

In the case where the acoustic wave is also driven by an external source \mathbf{F}_{ex} with wave vector \mathbf{k}_a and frequency ω_a , the equation for E_b becomes

$$\nabla \times (\nabla \times \mathbf{E}_b) - (\omega_b^2/c^2) [\boldsymbol{\epsilon}_b + 4\pi\boldsymbol{\kappa}_B \mathbf{E}_l \mathbf{E}_l^*] \mathbf{E}_b = - (4\pi\omega_b^2/c^2) i \mathbf{p} k_a \mathbf{E}_l \mathbf{F}_{\text{ex}}^* / (\omega_a^2 - \omega_a^0{}^2 - i2\omega_a \Gamma).$$

This equation will give a solution of \mathbf{E}_b whose amplitude will grow both parametrically and exponentially.

More generally, the electromagnetic fields should have an additional component at the vibrational frequency ω_v . The interaction Lagrangian L_{int} of Eq. (2) has an additional term $\boldsymbol{\gamma} \mathbf{Q}_s \cdot \mathbf{E}$. Consequently, the set of coupled-wave equations (5) and (6) should be modified accordingly, and joined by one more wave equation for $\mathbf{E}_v(\omega_v)$. Assuming $|E_l|$ constant, one still has four wave equations to be solved simultaneously. In infrared-inactive molecular crystals, the coupling parameter γ is small, so that $E_v(\omega_v)$ can usually be assumed absent. In polar crystals, however, γ is so large that one can solve the problem approximately in two steps. First, one assumes that the em wave and the vibrational wave at ω_v are coupled tightly together to form two waves of mixed character. Each of the latter is then coupled to the em waves at ω_s and ω_a to give the solution for the Stokes and anti-Stokes generation. We shall now proceed to the quantum description and show its equivalence to the classical description.

III. THE QUANTUM DESCRIPTION

The microscopic picture of the material system can only be described fully by the quantum theory. It is also possible to write the total Lagrangian density L or the corresponding total Hamiltonian \mathcal{H} in a completely quantized form,

$$\mathcal{H} = \mathcal{H}_{\text{elec}} + \mathcal{H}_{\text{rad}} + \mathcal{H}_{\text{vib}} + \mathcal{H}_{\text{int}}, \quad (13)$$

where the radiation and vibration fields are quantized through the use of creation and annihilation operators of photons and phonons. Loudon¹⁴ has studied the Raman scattering in this framework. He has used the eigenstates with prescribed numbers of photons and phonons. Then, since the uncertainty principle requires the phases of the fields to be completely undetermined, it would be impossible to describe amplification or attenuation of the fields through their mutual coupling. In order to regain the phase information in the quantum description, coherent states²⁴ for the photon and the phonon fields must be used. However, it has been shown by Glauber that when the number of quanta is large, the

coherent states become an exact analog of the classical waves.

In the semiclassical treatment, the photon and the phonon fields are described by waves. Only the electronic system is treated quantum mechanically. (The quantum states of the nucleus are neglected.) The Hamiltonian of Eq. (13) now reduces to

$$\mathcal{H} = \mathcal{H}_{\text{elec}} + \mathcal{H}_{\text{int}}, \quad (14)$$

with

$$\mathcal{H}_{\text{int}} = \mathcal{H}_{\text{e-r}} + \mathcal{H}_{\text{e-v}},$$

where $\mathcal{H}_{\text{e-r}}$ and $\mathcal{H}_{\text{e-v}}$ are the interaction Hamiltonians of the electronic and radiation systems and of the electronic and vibrational systems, respectively. We shall use the electric-dipole approximation so that

$$\mathcal{H}_{\text{e-r}} = -\mathbf{p} \cdot \sum_m \{ \mathbf{E}_m e^{-i\omega_m t} + \mathbf{E}_m^* e^{i\omega_m t} \}. \quad (15)$$

We also assume

$$\mathcal{H}_{\text{e-v}} = -\mathbf{f} \cdot \sum_m \{ \mathbf{Q}_m e^{-i\omega_m t} + \mathbf{Q}_m^* e^{i\omega_m t} \}. \quad (16)$$

The expectation values of the polarization \mathbf{p} and the generalized force \mathbf{f} can then be obtained from the density matrix formalism.²⁷ The linear part of $\langle \mathbf{f} \rangle$ is a measure of the elastic property of the medium, whereas the nonlinear part of $\langle \mathbf{f} \rangle$, proportional to powers of \mathbf{E} , is a measure of the photoelastic property of the medium. In this paper, we are particularly interested in the nonlinear part of $\langle \mathbf{p} \rangle$ and $\langle \mathbf{f} \rangle$.

We now consider the Raman scattering in a homogeneous medium with only first-order Stokes and anti-Stokes frequencies involved. The wave equations (5) and (6) are to be used with their right-hand sides replaced by $N \langle \mathbf{f}^{\text{NL}} \rangle$, $(4\pi\omega_s^2/c^2) N \langle \mathbf{p}_s^{\text{NL}} \rangle$, and $(4\pi\omega_a^2/c^2) \times N \langle \mathbf{p}_a^{\text{NL}} \rangle$, respectively. Let us first assume a two-level electronic system with the ground level $|g\rangle$ occupied and the excited level $|n\rangle$ empty. The density matrix elements of various orders can be obtained using a straightforward perturbation technique. Assume the matrix elements $\rho_{nn} = \rho_{gg} = 0$ and $\mathbf{f}_{ng} = 0$ and the frequencies $|\omega_{l,s,a} - \omega_{ng}|$, $\omega_v \gg$ linewidth. We find

$$\begin{aligned} \rho_{gg}^{(0)}(0) &= 1, \quad \rho_{nn}^{(0)}(0) = 0, \\ \rho_{ng}^{(1)}(\omega_{l,s,a}) &= \mathcal{H}_{ng}^{\text{er}}(\omega_{l,s,a}) / \hbar(\omega_{l,s,a} - \omega_{ng}), \\ \rho_{gn}^{(1)}(\omega_{l,s,a}) &= -\mathcal{H}_{ng}^{\text{er}}(\omega_{l,s,a}) / \hbar(\omega_{l,s,a} + \omega_{ng}), \\ \rho_{ng}^{(2)}(\omega_s) &= \mathcal{H}_{ng}^{\text{er}}(\omega_l) [\mathcal{H}_{nn}^{\text{ev}}(-\omega_v) - \mathcal{H}_{gg}^{\text{ev}}(-\omega_v)] / \\ &\quad \hbar^2(\omega_s - \omega_{ng})(\omega_l - \omega_{ng}), \\ \rho_{gn}^{(2)}(\omega_v) &= -\rho_{nn}^{(2)}(\omega_v) \\ &= (-1/\omega_v) \{ \mathcal{H}_{gn}^{\text{er}}(-\omega_s) \mathcal{H}_{ng}^{\text{er}}(\omega_l) A_{vs} \\ &\quad + \mathcal{H}_{gn}^{\text{er}}(-\omega_l) \mathcal{H}_{ng}^{\text{er}}(\omega_a) A_{va} \}, \\ A_{vs} &= \hbar^{-2} [(\omega_s - \omega_{ng})^{-1} - (\omega_l - \omega_{ng})^{-1} \\ &\quad + (\omega_s + \omega_{ng})^{-1} - (\omega_l + \omega_{ng})^{-1}], \\ A_{va} &= \hbar^{-2} [(\omega_l - \omega_{ng})^{-1} - (\omega_a - \omega_{ng})^{-1} \\ &\quad + (\omega_l + \omega_{ng})^{-1} - (\omega_a + \omega_{ng})^{-1}], \end{aligned} \quad (17)$$

²⁷ N. Bloembergen and Y. R. Shen, Phys. Rev. **133**, A37 (1964).

and similar expressions for $\rho_{gn}^{(2)}(\omega_s)$, $\rho_{ng}^{(2)}(\omega_a)$, and $\rho_{gn}^{(2)}(\omega_a)$.

To this second-order approximation, the expectation values of the nonlinear part of p and f are given by

$$\begin{aligned}\langle p_s^{NL} \rangle_i &= \text{Tr} p_s^i \rho^{(2)} = \xi_{sv}^{ijk} E_l^j Q_v^{k*}, \\ \langle p_a^{NL} \rangle_i &= \text{Tr} p_a^i \rho^{(2)} = \xi_{av}^{ijk} E_l^j Q_v^k, \\ \langle f_v^{NL} \rangle_i &= \xi_{vs}^{ijk} E_l^j E_s^{k*} + \xi_{va}^{ijk} E_l^j E_a^k,\end{aligned}$$

where

$$\begin{aligned}\xi_{vs}^{ijk}(\omega_s = \omega_l - \omega_v) &= \xi_{va}^{ijk}(\omega_v = \omega_l - \omega_s) \\ &= (\hat{p}_s^i)_{gn} (\hat{p}^j)_{ng} (f_{nn}^k - f_{gg}^k) A_{vs} / \omega_v, \\ \xi_{av}^{ijk}(\omega_a = \omega_l + \omega_v) &= \xi_{va}^{kji}(\omega_v = -\omega_l + \omega_a) \\ &= (\hat{p}_a^i)_{gn} (\hat{p}^j)_{ng} (f_{nn}^k - f_{gg}^k) A_{va} / \omega_v.\end{aligned}\quad (18)$$

The symmetry relations between ξ 's can be easily seen from a time-averaged energy expression,²⁸ the validity of which has been justified by Bloembergen.²⁹ We have

$$\langle F^{NL} \rangle = -2 \text{Re} \sum_{ijk} \{ \xi_1^{ijk} E_s^i E_l^j Q_v^{k*} + \xi_2^{ijk} E_a^i E_l^j Q_v^{k*} \}, \quad (19)$$

which leads immediately to the symmetric relations

$$\begin{aligned}\xi_{sv}^{ijk} &= \xi_1^{ijk} = \xi_{vs}^{kji}, \\ \xi_{av}^{ijk} &= \xi_2^{ijk} = \xi_{va}^{kji}.\end{aligned}\quad (20)$$

If the electronic system has more than two energy levels, then we need only to sum over the states in the expressions for ξ_{sv} and ξ_{av} , the sum over the ground states being properly weighted by the population distribution. The symmetry relations of course remain valid.

The microscopic expression for the Raman susceptibility can now be derived. In the absence of E_a , we have $\langle \mathbf{f}_v^{NL} \rangle = \xi_{vs} \mathbf{E}_l \mathbf{E}_s^*$ replacing $(\partial \alpha / \partial \mathbf{Q})_0 \mathbf{E}_l \mathbf{E}_s^*$ in Eq. (5). The Raman susceptibility in Eq. (7) then becomes

$$\chi_R^{ijmn} = -N^2 \sum_k \xi_{sv}^{ijk} \xi_{vs}^{kmn} / D^*. \quad (21)$$

We notice that the factor $\eta = (\mathbf{f}_{nn} - \mathbf{f}_{gg}) \cdot \mathbf{Q}_v / \hbar \omega_v$ is a measure of the perturbing strength of the vibrational wave on the electronic system. It is about the ratio of the deformation potential to the vibrational energy and hence is of the order of $\frac{1}{2} \sim \frac{1}{10}$. The linear polarizability of the system is given by

$$\begin{aligned}\alpha(\omega) &= \text{Tr} \mathbf{p} \mathbf{p}^{(1)}(\omega) / E(\omega) \\ &= \mathbf{p}_{ng} \mathbf{p}_{gn} [-1 / \hbar(\omega - \omega_{ng}) + 1 / \hbar(\omega + \omega_{ng})].\end{aligned}\quad (22)$$

Assuming $\omega_v \ll \omega_l \sim \frac{1}{2} \omega_{ng}$, we find $(\hat{p}_s)_{gn} (\hat{p}_l)_{ng} \hbar A_{vs} \sim \alpha_l / 10$. From the correspondence principle, we have $2N^{-1} \omega_v^2 Q_v^2 = \hbar \omega_v$. Equation (21) then gives a resonant Raman susceptibility of the form

$$\chi_R'' = N \eta^2 \alpha_l^2 / 100 \hbar \Gamma. \quad (23)$$

More generally, we should also find $\rho^{(3)}$. The calculation is straightforward, but the results are too complicated to be reproduced here. They give terms proportional to the third power of the wave amplitudes, but with nonresonant frequency denominators in the expressions of $\langle \mathbf{p}_s^{NL} \rangle$, $\langle \mathbf{p}_a^{NL} \rangle$, and $\langle \mathbf{f}_v^{NL} \rangle$. In keeping all fields, except E_l , only to the first power, Eq. (18) is generalized to the form

$$\begin{aligned}\langle \mathbf{p}_s^{NL} \rangle &= \xi_{sv} \mathbf{E}_l \mathbf{Q}_v + \xi_{ss} \mathbf{E}_l \mathbf{E}_l^* \mathbf{E}_s + \xi_{sa} \mathbf{E}_l \mathbf{E}_l \mathbf{E}_a^*, \\ \langle \mathbf{p}_a^{NL} \rangle &= \xi_{av} \mathbf{E}_l \mathbf{Q}_v + \xi_{aa} \mathbf{E}_l \mathbf{E}_l^* \mathbf{E}_a + \xi_{sa} \mathbf{E}_l \mathbf{E}_l \mathbf{E}_s^*, \\ \langle \mathbf{f}_v^{NL} \rangle &= \xi_{vs} \mathbf{E}_l \mathbf{E}_s^* + \xi_{va} \mathbf{E}_l^* \mathbf{E}_a + \xi_{vv} \mathbf{E}_l \mathbf{E}_l^* \mathbf{Q}_v.\end{aligned}\quad (24)$$

The term $\xi_{vv} \mathbf{E}_l \mathbf{E}_l^* \mathbf{Q}_v$ is essentially a saturation term and can often be neglected. We then have

$$Q_v = -N [\xi_{vs} E_l E_s^* + \xi_{va} E_l^* E_a] / D. \quad (25)$$

Substitution of \mathbf{Q}_v into $\langle \mathbf{p}_s^{NL} \rangle$ and $\langle \mathbf{p}_a^{NL} \rangle$ in Eq. (24) leads to the equations

$$\begin{aligned}\nabla \times (\nabla \times \mathbf{E}_s) - (\omega_s^2 \mathbf{e}_s / c^2) \mathbf{E}_s &= (4\pi \omega_s^2 / c^2) N \langle \mathbf{p}_s^{NL} \rangle, \\ \nabla \times (\nabla \times \mathbf{E}_a) - (\omega_a^2 \mathbf{e}_a / c^2) \mathbf{E}_a &= (4\pi \omega_a^2 / c^2) N \langle \mathbf{p}_a^{NL} \rangle,\end{aligned}\quad (26)$$

with

$$\begin{aligned}N \langle \mathbf{p}_s^{NL} \rangle &= (\chi_s + \chi_s^{\text{NR}}) \mathbf{E}_l \mathbf{E}_l^* \mathbf{E}_s + (\chi_{sa} + \chi_{sa}^{\text{NR}}) \mathbf{E}_l \mathbf{E}_l \mathbf{E}_a, & N \langle \mathbf{p}_a^{NL} \rangle &= (\chi_{as} + \chi_{as}^{\text{NR}}) \mathbf{E}_l \mathbf{E}_l \mathbf{E}_s^* + (\chi_a + \chi_a^{\text{NR}}) \mathbf{E}_l \mathbf{E}_l^* \mathbf{E}_a, \\ \chi_s &= -N^2 \xi_{sv} \xi_{vs} / D^* & \text{or} & \chi_s^{ijmn} = -N^2 \sum_k \xi_{sv}^{ijk} \xi_{vs}^{kmn} / D^*, \\ \chi_s^{\text{NR}} &= N \xi_{ss}, \\ \chi_{sa} &= -N^2 \xi_{sv} \xi_{va} / D^* & \text{or} & \chi_{sa}^{ijmn} = -N^2 \sum_k \xi_{sv}^{ijk} \xi_{va}^{kmn} / D^*, \\ \chi_{sa}^{\text{NR}} &= N \xi_{sa}, \\ \chi_{as} &= -N^2 \xi_{av} \xi_{vs} / D^* & \text{or} & \chi_{as}^{ijmn} = -N^2 \sum_k \xi_{av}^{ijk} \xi_{vs}^{kmn} / D, \\ \chi_a &= -N^2 \xi_{av} \xi_{va} / D & \text{or} & \chi_a^{ijmn} = -N^2 \sum_k \xi_{av}^{ijk} \xi_{va}^{kmn} / D, \\ \chi_a^{\text{NR}} &= N \xi_{aa}.\end{aligned}$$

²⁸ P. Pershan, Phys. Rev. **130**, 919 (1963).

²⁹ N. Bloembergen, *Nonlinear Optics* (W. A. Benjamin, Inc., New York, 1965).

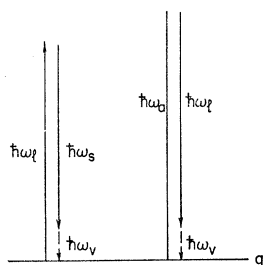


FIG. 1. Raman process in a model with the electronic system alone quantized.

the superscripts NR signifying the nonresonance nature of the corresponding susceptibilities. We notice that there is a complex symmetry relation

$$\chi_{sa}(\omega_s = 2\omega_l - \omega_a) = \chi_{as}^\dagger(\omega_a = 2\omega_l - \omega_s) \quad (27)$$

or in tensorial notation,

$$\chi_{sa}^{ijmn}(\omega_s = 2\omega_l - \omega_a) = \chi_{as}^{nmji^*}(\omega_a = 2\omega_l - \omega_s). \quad (28)$$

This is an illustration of the following rule which holds when the damping occurs in only one denominator of χ . When the interchange in frequencies involves a change of sign in the frequency combination which happens to be near resonance, the Hermitian conjugate of χ should be taken. In $\chi_{sa}(\omega_s = 2\omega_l - \omega_a)$, the near-resonance frequency appears as $\omega_l - \omega_a$, whereas in $\chi_{as}^\dagger(\omega_a = 2\omega_l - \omega_s)$, the near-resonance frequency is $\omega_l - \omega_s = -(\omega_l - \omega_a)$. Therefore, Eq. (28) follows. This symmetry relation is actually an application of Onsager's relationships, which may be based on the existence of a dissipation function, describing the steady-state loss. Pershan²⁸ has shown that the pure electric dipole susceptibilities are real in the nondissipative case. Their imaginary part describes loss. A symmetry relation, as in Eq. (28) represents therefore a connection between the free energy and the dissipation function. For the linear susceptibility, the connection between the real and the imaginary parts is embedded in the Kramers-Kronig relations. Our restriction that those nonlinear susceptibilities have only one complex denominator implies that they obey the same Kramers-Kronig relation as in the linear case. The complex permutation symmetry relation Eq. (28) is therefore similar to that in the linear case.

The imaginary part of χ_s and χ_a in Eq. (27) describes the Raman processes shown in Fig. 1. The real part of χ_s (or χ_a) describes a parametric process, the simultaneous scattering (in the loose sense)²⁷ of quanta at ω_l and ω_s (or ω_a). The interference of these scattering processes in a homogeneous medium leads to a change in index of refraction at ω_s proportional to $\mathbf{E}_l \mathbf{E}_l^*$ and vice versa.³⁰

The real part of χ_{sa} corresponds to a parametric process in which two quanta at ω_l scatter into a quantum at ω_s and one at ω_a , or vice versa. This leads to a para-

metric generation of ω_s and ω_a by the laser beam, or vice versa. The imaginary part of χ_{sa} can be described as the interference of the two Raman processes shown in Fig. 1. This interference may either enhance the generation of ω_s and the absorption of ω_a , or decrease the generation of ω_s and the absorption of ω_a . The relative phases of E_l , E_s , and E_a determine which situation applies. This shows that in order to see amplification or attenuation, the correct description is in terms of waves or coherent wave packets of oscillator states.

The terms χ^{NR} come from the third-order density matrix $\rho^{(3)}$. They involve only pure electric-dipole matrix elements with no resonance denominator, and are therefore real. The ratio of $|\chi^{\text{NR}}|$ to $|\chi_R''|$ is about 1/10 to 1. This is estimated as follows. The magnitude of χ_R'' gains a factor of $(\omega_l - \omega_{nq})/\Gamma$ over χ^{NR} through its resonance frequency denominator, but loses a factor of η^2 on the matrix elements. Moreover, χ^{NR} may have 100 times more terms than χ_R'' , These χ^{NR} terms give additional contributions to the parametric processes discussed before. The dispersion in these nonresonant susceptibilities may be ignored if the spacing to the excited electronic levels is much larger than the separation $\omega_a - \omega_s$. A single real χ^{NR} will suffice to describe this part of the nonlinear polarizations. A typical curve of $(\chi_s + \chi_s^{\text{NR}})$ versus frequency near resonance is shown in Fig. 2.

The usual quantum-mechanical description of Raman scattering is the process in which the material system absorbs a photon at ω_1 , emits a photon at ω_2 , and, makes a transition to some excited state at $\hbar(\omega_1 - \omega_2)$. The Raman susceptibility for the general two-level and three-level systems has been studied by the authors.²⁷ For Raman scattering in a molecular system, the final state in the process is usually a vibrational (and/or rotational) level. This model, in which the nuclear coordinates are also quantized, is related to the previous discussion in the following manner.

Consider $(\mathcal{H}_{\text{elec}} + \mathcal{H}_{\text{vib}})$ in Eq. (12) as a quantum system with the eigenstates represented by $|n, v\rangle$ where v designates the vibrational quantum number. In this sense, the vibrational waves appear as a fixed quantum state in the molecular system. The interaction Hamil-

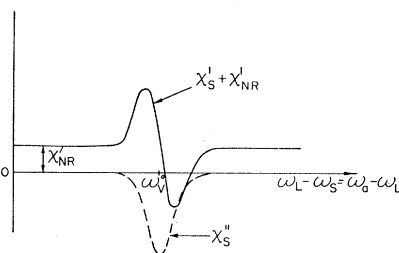


FIG. 2. Variation of Raman susceptibility with frequency $\omega_s + \Delta\omega$ near resonance ($\Delta\omega \sim 0$). Note that the Stokes frequency $\omega_s = \omega_l - \omega_v$ increases from right to left. The Kramers-Kronig relations are obeyed.

³⁰ R. D. Maker, R. W. Terhune, and C. W. Savage, Phys. Rev. Letters 12, 507, (1964).

tonian \mathcal{H}_{ev} acts as a perturbation in mixing different states $\langle n, v |$ and $\langle n', v' |$, and \mathcal{H}_{er} as a radiation perturbation on the system. In analogy to the two-level electronic system, we now assume a system with two pairs of levels, each electronic state $\langle n |$ being associated with two vibrational states $\langle v |$ and $\langle v' |$. With the same assumptions on

the matrix elements and frequencies, the susceptibilities can again be derived by using the density-matrix formulation. Since $\omega_a - \omega_l = \omega_l - \omega_s \approx \omega_{gv' - gv} \approx \omega_{nv' - nv}$, we keep in $\rho^{(2)}$ only the terms with a resonant denominator. The Raman susceptibility obtained from $\rho^{(3)}$ for the pure Stokes generation is given by

$$\chi_R = \frac{-N\hbar^{-3}}{\omega_l - \omega_s - \omega_{gv' - gv} - i\Gamma} \left| \frac{\langle gv' | p_s | nv \rangle \langle nv | p_l | gv \rangle}{\omega_l - \omega_{nv - gv}} + \frac{\langle gv | p_s | nv' \rangle \langle nv' | p_l | gv \rangle}{\omega_l - \omega_{nv' - gv}} \right. \\ \left. \frac{\langle gv' | p_l | nv \rangle \langle nv | p_s | gv \rangle}{\omega_s + \omega_{nv - gv}} - \frac{\langle gv | p_l | nv' \rangle \langle nv' | p_s | gv \rangle}{\omega_s + \omega_{nv' - gv}} \right|^2 \quad (29)$$

with $\langle gv | p | nv \rangle = \langle gv' | p | nv' \rangle = p_{gn}$. Taking into account the first-order perturbation of \mathcal{H}_{ev} , we have

$$\langle gv' | p | nv \rangle \cong -p_{gn} [(\mathcal{H}_{ev})_{nv' - nv} - (\mathcal{H}_{ev})_{gv' - gv}] / \hbar\omega_v = -\eta p_{gn}, \\ \langle gv | p | nv' \rangle \cong p_{gn} [(\mathcal{H}_{ev})_{nv - nv'} - (\mathcal{H}_{ev})_{gv - gv'}] / \hbar\omega_v = \eta p_{gn}, \quad (30)$$

where we assume that the only nonvanishing matrix elements are

$$\langle gv' | \mathcal{H}_{ev} | gv \rangle \neq \langle nv' | \mathcal{H}_{ev} | nv \rangle,$$

and

$$\omega_v = \frac{1}{2}(\omega_{nv' - nv} + \omega_{gv' - gv}) \approx \omega_{nv' - nv} \approx \omega_{gv' - gv}.$$

Substitution of Eq. (30) into Eq. (29) with the identity $2Q_v^2\omega_v^2N^{-1} = \hbar\omega_v$, leads to a Raman susceptibility identical to χ_R given in Eq. (21). The other susceptibilities in Eq. (27) can be derived in a similar manner. Here, the nonresonant terms in $\rho^{(2)}$ will lead to the nonresonant susceptibilities χ^{NR} . The details of the derivation are given in the book on nonlinear optics by Bloembergen.²⁹

With this model it is clear that at elevated temperatures, when the excited state $\langle g, v' |$ is also populated, the Raman susceptibilities should be multiplied by the population difference

$$(\rho_{gv, gv}^{(0)} - \rho_{gv', gv'}^{(0)}) / \text{Tr}\rho.$$

This factor arises only because of the existence of anharmonicity in the molecular vibration which is sufficiently large to cause transitions between higher vibrational states to be off resonance. For strictly harmonic oscillators, all vibrational transitions contribute and the temperature-dependent population factor would not occur in the susceptibility. This is just the case for the Brillouin effect, where the anharmonicity of acoustic vibration is negligible.

It is easy to generalize the discussion to include the rotational part of the molecular system. We can simply incorporate it into the electronic system, so that the combined system has rotation-electronic eigenstates. For the sake of simplicity, we shall omit the rotational part in our discussion.

To complete the quantum description, a few words should be said about the quantum nature of the damping constant Γ . In the linearized theory the inverse of Γ

represents the lifetime of a phonon. The evaluation of Γ has long been a well-known problem of dissipation in lattice. The phonon decays through the processes of phonon-phonon scattering, phonon-impurity scattering, and phonon-wall collision. In the case of long-wavelength optical phonons, the most important source of damping is the three- and four-phonon scattering processes via the anharmonic lattice potential. An optical phonon decays, during the process, into two or three phonons with lower energies. For the three-phonon process, Brout³¹ wrote down the general formulas for Γ as well as for the associated phonon frequency shift. Kleinman³² has calculated Γ for a simple ionic lattice with cubic anharmonic potential. In evaluating Γ , the most difficult part is to find the densities of states for the phonons involved. This is particularly true for a lattice with complicated molecules. In the latter case, a detailed quantitative calculation of Γ is quite difficult. Since the wavelength of light is much longer than the lattice constant, phonons with wave number $\mathbf{k}_l + \mathbf{k}_s$ and $\mathbf{k}_l - \mathbf{k}_s$ appear close to each other on the optical phonon branch. We would then expect that $\Gamma(\mathbf{k}_l + \mathbf{k}_s)$ and $\Gamma(\mathbf{k}_l - \mathbf{k}_s)$ are nearly equal.

IV. STIMULATED RAMAN AND BRILLOUIN SCATTERING

We have described stimulated Raman and Brillouin scattering as parametric processes resulting from coupling of light waves with vibrational waves. The coupled wave equations for the pure Stokes generation have been solved approximately in Sec. II. Actually, the wave vectors are functions of the nonlinear coupling and therefore cannot be prescribed. Here, we shall give a more rigorous solution to the problem.

For the Raman effect, the coupling between a Stokes

³¹ R. Brout, Phys. Rev. **107**, 664 (1957).

³² D. A. Kleinmen, Phys. Rev. **178**, 118 (1960).

to a very good approximation by dropping $(\Delta K)^2$ in the brackets,

$$\Delta K = \frac{1}{2} \left(\frac{i\alpha_s + D^*}{2\beta k_{vz}^0} \right) \pm \frac{1}{2} \left[\left(\frac{i\alpha_s - D^*}{2k_{vz}^0 \beta} \right)^2 + \frac{4\pi\omega_s^2 \lambda^2 |E_L|^2}{c^2 \beta k_{sz}^0 k_{vz}^0} \right]^{1/2}. \quad (36)$$

The corresponding waves are given by³³

$$E_s = C_{s+} \exp[i(k_{sz}^0 + \Delta K_+)z] + C_{s-} \exp[i(k_{sz}^0 + \Delta K_-)z], \quad (37)$$

$$Q_v^* = C_{v+} \exp[-i(k_{vz}^0 - \Delta K_+)z] + C_{v-} \exp[-i(k_{vz}^0 - \Delta K_-)z],$$

where the time factors $\exp(\pm i\omega t)$ are omitted,

$$C_{s\pm}/C_{v\pm} = (2\pi\omega_s^2/c^2 k_{sz}^0) \lambda E_L / (i\Delta K_{\pm} + \alpha_s). \quad (38)$$

For forward traveling Stokes waves, the boundary condition are $E_s(z=0) = \mathcal{E}_s$ and $Q_v(z=0) = 0$. We find

$$C_{s+} = [(\Delta K_- - i\alpha_s) / (\Delta K_- - \Delta K_+)] \mathcal{E}_s, \quad (39)$$

$$C_{s-} = [(\Delta K_+ - i\alpha_s) / (\Delta K_+ - \Delta K_-)] \mathcal{E}_s. \quad (40)$$

In general, the quartic characteristic equation (33) or (35) leads to four composite Stokes-vibrational waves propagating in the Raman medium, two traveling forward and two backward. Each composite wave consists of a Stokes and a vibrational component with their amplitude ratio fixed. A more rigorous way of describing the problem is as follows. The Raman medium is a slab of length L bounded by different media on the two sides, and is made active by the laser beam propagating across the medium. A pure Stokes wave and a pure vibrational wave incident on the medium give rise to a pure Stokes and a pure vibrational waves reflected from the first boundary surface, two forward-traveling composite waves and two backward-traveling composite waves in the medium, and a pure Stokes and a pure vibrational wave transmitted from the second boundary surface. The amplitudes of all these waves can be found in terms of the amplitudes of the incident waves through two boundary conditions for the Stokes waves and two boundary conditions for the vibrational waves at each boundary. The problem is then completely solved. The reflection and transmission coefficients for the Stokes and vibrational waves at the boundaries can be calculated. They are different from those obtained when either the Stokes or the vibrational wave alone is present because of the coupling between the two waves. However, in cases where the vibrational wave in the Raman medium is heavily damped, the composite waves are either almost purely Stokes or almost purely vibrational. One would then find that the reflection and transmission coefficients are not far from those for the pure wave case. When the reflection coefficients at the boundaries in the Raman medium are so small that the Barkhausen condition for

sustained oscillation is not reached, one can normally treat the forward and backward waves in the medium separately. Here, in the text, we assume that the reflection coefficients are very small so that the feedback can be neglected. The calculation can be extended to the case of multiple reflections in the manner indicated.

Assume

$$|D^*/2k_{vz}^0 \beta|^2 \gg (4\pi\omega_s^2 \lambda^2 |E_L|^2 / c^2 \beta k_{sz}^0 k_{vz}^0),$$

or at resonance

$$\Gamma \gg (g_s/k_{vz}^0)(2\beta k_{vz}^0 / \omega_v),$$

where $g_s = 2\pi\omega_s^2 \lambda^2 |E_L|^2 / c^2 k_{sz}^0 \omega_v \Gamma$. This corresponds to a vibrational wave of large damping. The square root in Eq. (36) may be expanded to give roots. One root is $\Delta K_- \simeq D^*/2k_{vz}^0 \beta$, whose corresponding wave has almost pure vibrational character but is highly damped. We note that for $\beta \rightarrow 0$, the wave has infinite attenuation. This is the case of isolated molecules whose vibration cannot be propagated. The other root is

$$\Delta K_+ \simeq i\alpha_s - \frac{1}{2} i g_s (-i2\omega_v \Gamma / D^*) + 2g_s^2 \beta k_{vz}^0 \omega_v^2 \Gamma^2 / D^{*3}. \quad (41)$$

The corresponding wave has almost pure electromagnetic character. When α_s is sufficiently small, this gives amplification to the Stokes wave since $\text{Im}(\Delta K_+) < 0$.

In this approximation, we have $|\Delta K_-| \gg |\Delta K_+| > \alpha_s$. For the forward-traveling Stokes wave, since $\text{Im}(\Delta K_-) > 0$ and $\text{Im}(\Delta K_+) < 0$, we have essentially

$$E_s \simeq \mathcal{E}_s \exp[i(k_{sz}^0 + \Delta K_+)z] \quad (42)$$

at a distance $z \gg 1/\text{Im}(\Delta K_-)$. Similarly, for the backward-traveling Stokes wave, we have, with $k_{sz}^0, \alpha_s < 0$,

$$E_s \simeq \mathcal{E}_s \exp[i(k_{sz}^0 + \Delta K_+)(z-L)] \quad (43)$$

at a distance $|z-L| \gg 1/\text{Im}(\Delta K_-)$.

If only the first-order term in Eq. (41) is taken, we see immediately that ΔK_+ agrees with the Raman susceptibility in Eq. (7). This proves that the approximation in Sec. II is valid if the vibrational wave is highly damped. To this approximation, the backward-traveling wave has exactly the same gain constant as the forward-traveling wave if the k_v dependence in Γ can be neglected. However, on the basis of a general consideration of the available volume in the momentum space for the final phonon state, one would expect $\Gamma(k_v) = \Gamma_0 + Ck_v^2$ with $C > 0$. A phonon with a wave vector $k_i + k_s$ is slightly more damped than a phonon with $k_i - k_s$. A difference of a few percent in the gain should be sufficient to give a large forward-backward ratio of intensities since the total power amplification usually observed is of the order of $e^{20} \sim e^{30}$. This forward-backward ratio depends exponentially on the laser intensity. If the second-order term in Eq. (41) is taken into account, the forward-traveling wave has an additional gain per centimeter of

³³ N. M. Kroll, J. Appl. Phys. (to be published).

$g_s^2\beta(k_{vz}^0)_f/4\omega_v\Gamma_f$ and the backward traveling wave has an additional attenuation of $g_s^2\beta(k_{vz}^0)_b/4\omega_v\Gamma_b$. This also leads to a forward-backward asymmetry depending exponentially on the square of the laser intensity. The ratio of this second-order gain to the first-order gain is $g_s\beta(k_{vz}^0)_b/2\omega_v\Gamma$, which is of the order of $g_s/(k_{vz}^0)_b$ if $\beta(k_{vz}^0)_b^2 \sim 2\omega_v\Gamma$. This would be too small to give any appreciable forward-backward asymmetry if $g_s \ll (k_{vz}^0)_b/100$.

Let \mathcal{E}_0 be the amplitude of the incoming wave at ω_s , and T and T' be the transmitting coefficients of the Stokes wave from the surrounding into the medium and from the medium into the surrounding, respectively. Then, if the medium has a length L with $L \gg \omega_v\Gamma/\beta k_{vz}^0$, we have a Stokes amplitude of $\mathcal{E}_0 T T' \exp[\text{Im}(\Delta K_+)l]$ emerging from the medium after a single traversal across the medium. In the absence of an incoming wave, the Stokes intensity is built up from noise or the zero-point fluctuations. The noise photon density per steradian in $\Delta\nu = c$ cps at $\lambda = 6943 \text{ \AA}$ is 10^8 photons/cm³. In the case of Raman lasers, the oscillation will start from noise when the Barkhausen condition is satisfied.

$$R_1 R_2 \exp[i2k_{sz}' + i(\Delta K_f - \Delta K_b)]d = 1, \quad (44)$$

where R_1 and R_2 are complex reflection coefficients of the two mirrors, d is the length of the cell, and ΔK_f and ΔK_b are given in Eq. (37) for forward and backward traveling Stokes waves. The real and imaginary parts of Eq. (44) determine the threshold value for $|E_l|^2$ and the frequency of oscillation. For the rather broad natural Raman lines, the frequency is essentially determined by the mirror separation d . If the Raman cavity is inside the cavity of the laser, then two oscillation conditions, for ω_l and ω_s , respectively, should be satisfied simultaneously. The phase of the Stokes wave is not known *a priori*. As the wave builds up, and is fed back by reflection, a definite but unknown phase is established. Through multiple reflections in the cavity, the Stokes wave will finally deplete the laser power and reach the point of saturation.

The large damping of the vibrational wave leads to the Raman susceptibility of Eqs. (7) or (21). In general, χ_{Raman} is a tensor. For isotropic media, however, it has only two independent elements. The nonlinear polarization at the Stokes frequency takes the form

$$(P_s^{\text{NL}})_i = N \langle p_s^{\text{NL}} \rangle = \chi_{ijij}(E_l^*)_j (E_s)_i (E_l)_j + \chi_{iijj}(E_l^*)_i (E_s)_j (E_l)_j. \quad (45)$$

The first term imposes no restriction on the polarization of \mathbf{E}_s , but the second term requires \mathbf{E}_s parallel to \mathbf{E}_l . Experiments^{34,35} have shown that the Stokes wave is almost completely polarized in the direction of polarization of \mathbf{E}_l . This suggests that χ_{ijij} must be smaller than χ_{iijj} . Even a difference of 50% or less between them can

cause complete polarization of the experimentally observed intensity, since the χ 's occur in the exponent of the gain factor.

The Brillouin scattering is closely analogous to the Raman scattering except that the dispersion of the acoustic waves which take over the role of optical phonon waves in the Raman effect, is normal. The coupled wave equations take the form

$$C_a \nabla^2 \mathbf{A}^* + (\omega_a^2 \rho - i2\omega_a \rho \Gamma) \mathbf{A}^* = +\lambda \mathbf{E}_l^* \mathbf{E}_b, \\ \nabla \times (\nabla \times \mathbf{E}_b) - (\epsilon_b \omega_b^2 / c^2) \mathbf{E}_b = (4\pi \omega_b^2 / c^2) \lambda^* \mathbf{E}_l \mathbf{A}^*, \quad (46)$$

where

$$\lambda = ik_a \mathbf{p}, \\ \mathbf{E}_l = \mathbf{E}_l \exp[i(\mathbf{k}_l \cdot \mathbf{r} - \omega_l t)], \\ \omega_l = \omega_b + \omega_a.$$

The solution is again obtained in the form of waves,

$$\mathbf{E}_b = \mathbf{E}_b \exp[i(\mathbf{k}_b \cdot \mathbf{r} - \omega_b t)], \quad k_b = k_b' + ik_b'' \\ \mathbf{A} = \mathbf{A} \exp[i(\mathbf{k}_a \cdot \mathbf{r} - \omega_a t)], \quad k_a = k_a' + ik_a''. \quad (47)$$

\mathbf{E}_l , \mathbf{E}_b , and \mathbf{A} being all linearly polarized and k_a' and k_b' satisfying the matching condition $\mathbf{k}_a' + \mathbf{k}_b' = \mathbf{k}_l$. Since the acoustic frequency is very small compared to the light frequency, $|k_b'| \approx |k_l|$. This leads to the Brillouin relation for light scattered at an angle θ with the wave vector \mathbf{k}_l .

$$2k_l \sin(\theta/2) = k_a$$

or

$$\omega_a = 2\omega_l(v/c) \sin(\theta/2), \quad (48)$$

where (v/c) is the ratio of the phase velocities of sound and light in the medium. Therefore, the maximum frequency shift in the Brillouin scattering is in the backward direction.

The wave equations can be solved in complete analogy to the case of Raman scattering. We simply make the following correspondence between Eqs. (31) and (46):

$$\beta \leftrightarrow -C_a/\rho, \quad k_v^{02} = (\omega_0^2 - \omega_v^{02})/\beta \leftrightarrow k_a^{02} = \omega_a^{02} \rho/C_a, \\ Q_v \leftrightarrow \rho^{1/2} A, \quad \omega_v \Gamma \leftrightarrow \omega_a \Gamma, \quad \text{and} \quad \lambda^2 \leftrightarrow |\lambda|^2/\rho^{1/2}.$$

When the acoustic wave is highly damped such that $\Gamma \gg [4\pi\omega_b^2 |\lambda|^2 |E_l|^2 / c^2 \rho k_{bz}^0 k_{az}^0]^{1/2}$, the gain per unit length of the Brillouin scattered wave at resonance is, to the first order, $|\Delta K| \simeq \pi\omega_b^2 \rho^2 k_a^2 |E_l|^2 / \omega_v \Gamma c^2 k_{bz}^0 \rho - \alpha_b$, which is in complete agreement with the Brillouin susceptibility in Eq. (11). The amplitude ratio $|E_b/A|$ is $2\omega_a \rho \Gamma / E_l \rho k_a$. In crystals and fluids at room temperature, the acoustic damping is much larger than the damping of light waves α_b in a transparent medium. A typical attenuation coefficient for an ultrasonic wave at 300°K is $\alpha_a = 400 \text{ cm}^{-1}$ at 10^{10} cps. α_a increases as the square of the frequency. The light attenuation is $\alpha_b \ll 0.1 \text{ cm}^{-1}$. One may thus expect the above approximation to be valid. However, as the temperature is lowered, α_a may gradually reduce to a small value comparable to α_b . Then the exact solution of Eq. (46)

³⁴ R. W. Terhune (to be published).

³⁵ G. Bret and G. Mayer, *Compt. Rend.* **258**, 3265 (1964).

must be used.

$$\Delta K = +\frac{1}{2}i \left(\alpha_b - \frac{\rho D^*}{2k_{az}^0 C_a} \right) \pm \frac{1}{2} \left[\left(i\alpha_b + \frac{\rho D^*}{2k_{az}^0 C_a} \right)^2 - \frac{4\pi\omega_s^2 p^2 k_a^2 |E_l|^2}{c^2 C_a k_{az}^m k_{bz}^m} \right]^{1/2}, \quad (49)$$

$$D^* = \omega_v^2 - (C_a/p)k_a^0{}^2 - i2\omega_v\Gamma$$

which corresponds to waves with mixed light and acoustic character.

The stimulated Brillouin effect has been observed by Chiao, Townes, and Stoicheff¹⁰ in quartz and sapphire. The backward scattered light, which has the maximum frequency shift and probably the lowest threshold because of the longer path length of interaction with the laser beam, was detected. A fraction of ω_a/ω_l of the laser power is converted into ultrasonic power and then into heat by a damping mechanism. Immediately above threshold, the laser power is depleted and converted to the Brillouin shifted frequency (see Sec. VI). This limits other processes with higher threshold. The nonlinear nature of the problem is such that only a few processes with the lowest threshold will go. The Brillouin scattering is in competition with the Raman scattering. It is noteworthy in this respect that quartz and sapphire have not shown the stimulated Raman effect, while calcite which exhibits the latter effect does not show stimulated Brillouin scattering. However, it is also possible that stimulated Raman and Brillouin effects appear simultaneously because of the multimode structure of the laser beam.

The stimulated Raman and Brillouin effects are in close analogy to the process of parametric down conversion. In the latter case, the phonon wave equation is replaced by another em wave equation. The pump field is at ω_l . The two coupled waves are at the signal frequency ω_s and at the idler frequency ω_i , with $\omega_l = \omega_s + \omega_i$, and $\mathbf{k}_l = \mathbf{k}_s' + \mathbf{k}_i'$. With proper substitution of the physical quantities, all formulas remain valid in this case. In particular, when the damping of the idler wave is much larger than that of the signal wave, and if the latter is sufficiently small, there will always be gain in the signal wave, even though the other wave is strongly attenuated. The amplified wave has almost pure ω_s character. A wave at ω_i with much smaller amplitude is however dragged along.

V. COUPLING BETWEEN STOKES AND ANTI-STOKES WAVES

In the last section, we have deliberately assumed the absence of anti-Stokes waves. The real situation is however that the anti-Stokes wave is always present and coupled to the Stokes and vibrational waves. Even in a Raman laser, a small amount of anti-Stokes wave is always dragged along with the Stokes wave in the

forward direction. For certain directions, the coupling between these waves appears to be very strong, and the assumption of the absence of anti-Stokes waves breaks down. In general, one would think that waves at the vibrational frequency ω_v , the laser frequency ω_l , and combination frequencies $\omega_l \pm n\omega_v$ should be all coupled together. Under certain conditions discussed in the next section, these higher order Stokes and anti-Stokes waves may be omitted. The problem can be further simplified by assuming highly damped phonon waves. The approximation in Sec. II can be used and the wave equation at ω_v can thus be eliminated.

The generation or amplification of waves at ω_s and ω_a is obtained from the solution of wave equations (26). We assume that the medium is isotropic and that all waves are polarized in the same direction. The non-resonant susceptibilities are now taken into account, but their dispersion may be ignored. The coupled-wave equations can be written in the form,

$$\begin{aligned} \nabla^2 E_s - \frac{\epsilon_s}{c^2} \frac{\partial^2}{\partial t^2} E_s &= \frac{4\pi}{c^2} \frac{\partial^2}{\partial t^2} \{ (\chi_s + \chi_{NR}) |E_l|^2 E_s \\ &\quad + [(\chi_s \chi_a^*)^{1/2} + \chi_{NR}] E_l^2 E_a^* \}, \\ \nabla^2 E_a^* - \frac{\epsilon_a^*}{c^2} \frac{\partial^2}{\partial t^2} E_a^* &= \frac{4\pi}{c^2} \frac{\partial^2}{\partial t^2} \{ [(\chi_a^* \chi_s)^{1/2} + \chi_{NR}] \\ &\quad \times E_l^* E_s + (\chi_a^* + \chi_{NR}) |E_l|^2 E_a^* \}, \end{aligned} \quad (50)$$

where the laser field is assumed to be constant and described by $\mathbf{E}_l = \mathbf{E}_l \exp[i(\mathbf{k}_l \cdot \mathbf{r} - \omega_l t)]$.

The plane boundary at $z=0$ requires the solution to be in the form of plane waves with constant amplitudes in planes parallel to the boundary.

$$\begin{aligned} E_s &= \mathcal{E}_s \exp(ik_{sx}x + ik_{sy}y) \exp(ik_{sz}z - i\omega_s t), \\ E_a &= \mathcal{E}_a \exp(ik_{ax}x + ik_{ay}y) \exp(ik_{az}z - i\omega_a t), \end{aligned} \quad (51)$$

with $\mathbf{k}_s + \mathbf{k}_a = 2\mathbf{k}_l$ and $\omega_s + \omega_a = 2\omega_l$. Substitution of these expressions into the wave equations reduces the problem to an eigenvalue equation, which is quartic in k_{sz} , if k_{sx} , k_{sy} , and ω_s are prescribed. The problem is to determine how the gain, signified by k_{sz}'' , varies as a function of the frequency ω_s , and the direction of the outgoing wave, determined by $(k_{sx}^2 + k_{sy}^2)^{1/2}$.

Introduce the new notation

$$\begin{aligned} (k_s^0)^2 &= \epsilon_s' \omega_s^2 / c^2, \\ (k_a^0)^2 &= \epsilon_a' \omega_a^2 / c^2, \\ k_{sz}^m &= (k_s^0{}^2 - k_{sx}^2 - k_{sy}^2)^{1/2}, \\ k_{az}^m &= (k_a^0{}^2 - k_{ax}^2 - k_{ay}^2)^{1/2} \\ &= \{ k_a^0{}^2 - (2k_{lx} - k_{sx})^2 - (2k_{ly} - k_{sy})^2 \}^{1/2}, \quad (52) \\ \Delta k &= 2k_{lz} - k_{sz}^m - k_{az}^m \ll k_{sz}, \\ \Delta K &= k_{sz} - k_{sz}^m, \\ \alpha_s &= \omega_s^2 \epsilon_s'' / 2c^2 k_{sz}^m, \\ \alpha_a &= \omega_a^2 \epsilon_a'' / 2c^2 k_{az}^m. \end{aligned}$$

\mathcal{E}_{s0} and \mathcal{E}_{a0}^* being the boundary values of E_s and E_a^* at $z=0$.

We are particularly interested in the part which shows exponential gain for the waves. The gain coefficient $\text{Im}(\Delta K_1)$ and the wave amplitudes $|E_s|$ and $|E_a^*|$ are functions of both the direction of the outgoing wave and its frequency offset from exact resonance. The deviation from the direction of linear momentum matching is determined by Δk through the vector diagram in Fig. 5. This quantity can be normalized by division by the Stokes power gain per unit length $g_s = (4\pi\omega_s^2/c^2 k_{sz}^m) \times |\chi_s''| |E_l|^2$. The frequency offset $\Delta\omega = \omega_l - \omega_s - \omega_v^0$ may be normalized by division by the damping constant or the half-linewidth of the vibrational level Γ . A choice for the nonresonant part of the susceptibility is made $\chi_{NR} = 0.1 |\chi_s''|_{\max}$. A machine calculation then gives the gain constant ΔK . For fixed $\Delta\omega$, a typical curve of $I_a \sim |E_a|^2$ versus Δk is shown in Fig. 6. It shows a dip around $\Delta k=0$ and two peaks at the sides. The dip corresponds to no generation or amplification of Stokes and anti-Stokes waves in the momentum matching direction. As $\Delta\omega$ varies from positive to negative, the left peak first increases, reaches a maximum at some positive $\Delta\omega$, and then decreases rapidly to small values as $\Delta\omega$ becomes more and more negative. The right peak, however, first increases rapidly, reaches the maximum at some negative $\Delta\omega$, and then decreases rather slowly. The two peaks are about at the same height when $\Delta\omega/\Gamma \approx 0.1$.

The spectral distribution and the angular distribution of the anti-Stokes intensity are obtained from partial integration of $|E_a|^2$ over Δk and $\Delta\omega$, respectively. They can be seen roughly from Figs. 7 and 8. In Fig. 7 the anti-Stokes intensity I_a is plotted against $\Delta\omega$, the momentum mismatch Δk being chosen to maximize I_a for each value of $\Delta\omega$. In Fig. 8, the anti-Stokes intensity I_a is maximized by $\Delta\omega$ for each value of Δk and plotted against Δk . The corresponding curve of the gain coefficient $|\text{Im}\Delta K_1|$ versus Δk is given in Fig. 9. Because of the presence of χ_{NR} , the curves appear to be asymmetric. The optimum anti-Stokes intensity occurs at $\Delta k/g_s \approx 2$ and $-\Delta\omega/\Gamma \approx 0.25-0.30$ in our examples. The wave direction corresponding to a given Δk is found from Eq. (40) and Fig. 5. The deviation of the direction of optimum gain from the direction θ_0 for perfect linear momentum matching is thus determined. Corresponding to this direction θ_0 , the dip in the gain curve gives rise to a dark ring in the directional intensity pattern of the Stokes radiation. There should be a bright ring for the anti-Stokes radiation in a direction with an offset from the phase-matched direction. Within the sharp bright ring, there should also be a dark ring corresponding to the dip at the linear phase-matched direction. This, however, may not be seen in the real experiments because of the geometric limitation and the photographic sensitivity.

A small fraction of the intensity in any direction

should be at the anti-Stokes frequency. The ratio of the intensities of coupled Stokes and anti-Stokes radiation is given in Eq. (59). It should be emphasized that these results are derived for the condition that the laser field can be considered as a constant parameter and is not depleted. This condition is not satisfied in the usual experiments on coherent Raman generation. The saturation effect will be dealt with in the following section. A comparison with the experimental results is postponed till Sec. IX.

We have simplified the problem by assuming that the vibrational wave is highly damped. More rigorously, we should have solved the three coupled wave equations exactly, two for the light waves at ω_s and ω_a , and one for the vibrational wave at ω_v . In the case of polar crystals treated by Loudon,¹⁴ we have also wave equations for the em wave at ω_v . Then the most rigorous way of solving the problem is to solve all the coupled wave equations together. The approximation method, is however, to assume that the em wave and the vibrational wave at ω_v are tightly coupled and the resulting mixed wave highly damped. Only the coupled wave equations at ω_s and ω_a are thus left to be solved.

The above discussion is not restricted to light waves and acoustic waves. The interaction between light waves and spin waves, and between electromagnetic waves and electron density and velocity waves, could be treated along similar lines.^{37,38}

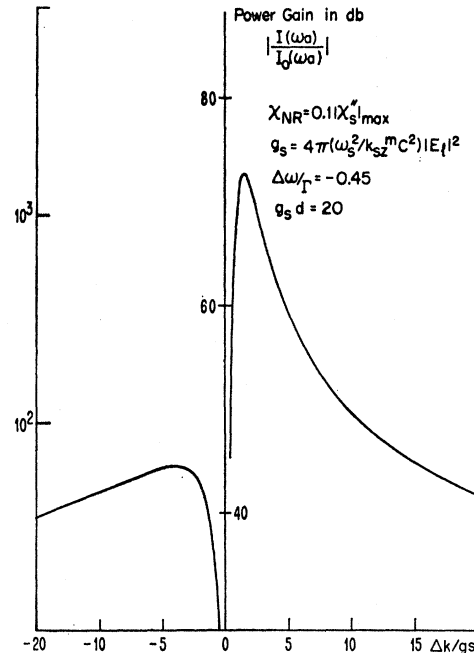


FIG. 6. A typical curve of anti-Stokes intensity versus the momentum mismatch Δk for fixed frequency offset $\Delta\omega$. All the quantities are properly normalized.

³⁷ P. K. Tien and H. Suhl, Proc. IRE 46, 700 (1958).

³⁸ J. R. Pierce, *Travelling Wave Tubes* (D. Van Nostrand Company, Princeton, New Jersey, 1950).

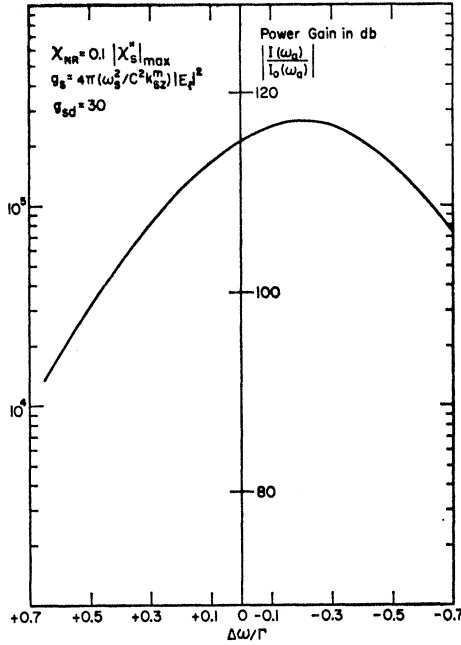


FIG. 7. Anti-Stokes intensity versus the frequency offset $\Delta\omega$, (normalized by the linewidth Γ), the linear momentum mismatch Δk being chosen to maximize the intensity for each value of $\Delta\omega$. The asymmetry is due to the nonresonant part $\chi_{NR} = 0.1 |\chi_s''|_{max}$.

VI. THE SATURATION EFFECT

In the stimulated Raman effect, the laser pump field is the energy source. Through nonlinear coupling among waves, its energy is transferred to the Raman radiation and the phonon wave. It is correct to say that the laser field is approximately a constant only when the Raman radiation is weak. The Raman radiation first increases exponentially and the nonlinear coupling between the waves increases proportionally. When the Raman intensity is sufficiently high, the nonlinear coupling also becomes so large that the laser power is now drained into Raman radiation at an extremely fast rate, and would be completely converted if the coupling always existed.

The Raman radiation can in turn act as a source in generating higher order Stokes and anti-Stokes radiation. In principle, all waves at frequencies ω_l , ω_s and $\omega_l \pm n\omega_s$ are coupled at the same time. The complete set of coupled-wave equations must be solved. The wave equation at ω_s can be eliminated because the wave is highly damped, the energy of the optical phonon wave being converted into heat through damping. In the energy consideration, the anti-Stokes waves can also be neglected, since they are highly directional. We are therefore left with a set of coupled-wave equations at the Stokes and laser frequencies only.

To the degree of approximation that the Stokes waves are assumed all propagating in the z direction, the set of coupled energy equations can be written in the

form

$$\begin{aligned} dP_l/dz &= -\lambda_0 P_{s1} P_l - \beta_0 P_l, \\ dP_{s1}/dz &= \lambda_1 P_{s1} P_l - \lambda_1' P_{s1} P_{s2} - \beta_1 P_{s1}, \\ dP_{s2}/dz &= \lambda_2 P_{s1} P_{s2} - \lambda_2' P_{s2} P_{s3} - \beta_2 P_{s2}, \end{aligned} \tag{60}$$

where

$$\begin{aligned} \lambda_0 &= 16\pi^3 \omega_l^2 \chi_{s1}'' / c^3 k_l, \\ \lambda_1 &= (\omega_{s1}^2 k_l / \omega_l^2 k_{s1}) \lambda_0, \\ \lambda_1' &= (\omega_{s2}^2 k_l / \omega_l^2 k_{s1}) (\chi_{s2}'' / \chi_{s1}'') \lambda_0, \\ \lambda_2 &= (\omega_{s2}^2 k_l / \omega_l^2 k_{s2}) (\chi_{s2}'' / \chi_{s1}'') \lambda_0, \\ \lambda_2' &= (\omega_{s2}^2 k_l / \omega_l^2 k_{s2}) (\chi_{s3}'' / \chi_{s1}'') \lambda_0, \text{ etc.} \end{aligned}$$

χ_{s1}'' , χ_{s2}'' , $\chi_{s3}'' \dots$ are the resonant Raman susceptibilities for first-order, second-order, third-order, \dots , Stokes waves, respectively; P 's and β 's are the power and loss coefficients for these waves.

We shall assume that the fifth and higher order Stokes waves are suppressed, and that the Stokes waves are built up from noise. The set of five equations is then solved by machine calculation. The case of nitrobenzene with boundary conditions $P_{s1}(0)/P_l(0) = P_{s2}(0)/P_l(0) = P_{s3}(0)/P_l(0) = P_{s4}(0)/P_l(0) = 3.6 \times 10^{-12}$ is chosen as an example. The result is shown in Fig. 9, where the powers P 's are normalized by $P_l(0)$, the loss coefficient β 's normalized by $\lambda_0 P_l(0)$, and the distance z is replaced by the dimensionless one $Z = \lambda_0 P_l(0) z$.

The result of Fig. 10 is rather unexpected. At any fixed distance z , there are at most two waves with appreciable intensity. All the other waves are smaller by several orders of magnitude. Except for some narrow overlapping regions, there is essentially only one single wave present. Had it not been for the presence of loss

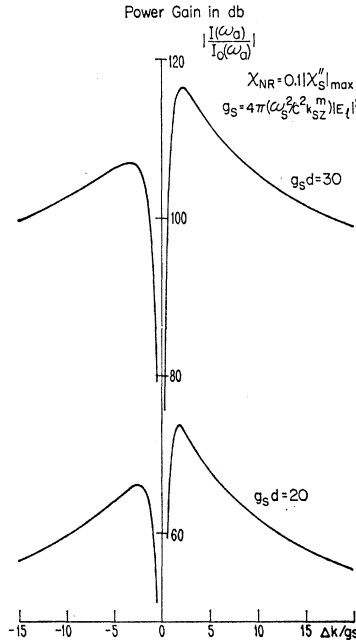


FIG. 8. Anti-Stokes intensity versus the linear momentum mismatch Δk (normalized by the Stokes power gain g_s) the frequency offset $\Delta\omega$ being chosen to maximize the intensity for each value of Δk . The asymmetry is due to $\chi_{NR} = 0.1 |\chi_s''|_{max}$.

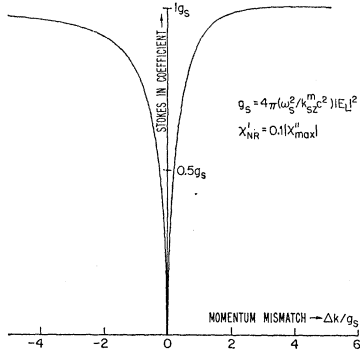


FIG. 9. The Stokes power gain as a function of the normalized linear momentum mismatch $\Delta k/g_s$ in the z direction, the frequency offset $\Delta\omega$ being chosen to maximize the gain. The asymmetry is due to the nonresonant part $\chi_{NR} = 0.1|\chi_s''|_{\max}$.

factors β , the number of photons would always remain constant. In the overlapping regions, the intensity of one wave decreases rapidly, converting most of its power to the next higher order Stokes wave and the remaining part to phonons. Therefore, in the practical sense, we can speak of the laser power as constant in a definite region. Then as z increases further, it is suddenly depleted completely, whereas the first Stokes power builds up to its maximum. The first Stokes power remains constant for a certain distance and then converts again to second Stokes power, and so on. Finally, if z is sufficiently large, most of the laser power would be converted into phonons or heat.

This shows that our discussion in the last section is approximately valid as long as the laser power is not depleted very much. In that case, the laser power can be regarded as a constant and the higher order Raman radiation as absent. We have however assumed that the laser beam has a single mode and a uniform intensity over the whole cross section. In practice, the assumption can hardly be fulfilled. This may complicate the problem greatly, especially if the mode structure and the intensity distribution of the laser beam are unknown. For different modes with different intensities, the normalized distance Z is different, so that when the laser beam is strong, Stokes waves of several orders can be generated simultaneously at the same z . That the laser intensity can only be uniform over a small cross section also makes our infinite plane-wave analysis at most a crude approximation to the real experiments reported so far.

We now discuss how the amplification of coupled Stokes and anti-Stokes waves is changed when the laser power is depleted. We can simplify the problem by assuming that the laser intensity varies as

$$\begin{aligned} |E_l|^2 &= |E_l(0)|^2, & 0 \leq z \leq z_0, \\ &= |E_l(0)|^2 \exp(-gz), & z \geq z_0. \end{aligned} \quad (61)$$

Then take the solution of Eq. (38) to be of the form

$$\begin{aligned} E_s &= \mathcal{E}_s \exp(ik_{sx}x + ik_{sy}y) \exp[i\varphi_s(z) - i\omega_s t], \\ E_a^* &= \mathcal{E}_a^* \exp(-ik_{ax}x - ik_{ay}y) \exp[-i\varphi_a^*(z) + i\omega_a t]. \end{aligned}$$

If $(1/k_s^0)(\partial^2 \varphi_s / \partial z^2) \ll \partial \varphi_s / \partial z$ and $(1/k_a^0)(\partial^2 \varphi_a / \partial z^2) \ll \partial \varphi_a / \partial z$ we can use the approximation method similar to the WKB method. When the notation of Eq. (52) is used, the determinantal equation (53) is obtained with Δk replaced by $(\partial \varphi_1 / \partial z)$ where $\partial \varphi_1 / \partial z = \partial \varphi_s / \partial z - k_{sz}^m$. Since $|\partial \varphi_1 / \partial z| \ll k_{sz}^m$, we get

$$\begin{aligned} \varphi_1(z) &= \left(\frac{1}{2}\Delta k + i\alpha_{sa}\right)z \pm \int_0^z \left\{ \frac{1}{4}(\Delta k^2) \right. \\ &\quad \left. - (2\pi\omega_s^2/c^2 k_{sz}^m)(\chi_s + \chi_{NR})|E_l|^2 \Delta k \right\}^{1/2} dz, \end{aligned}$$

which can be integrated easily when the expression of $|E_l|^2$ is substituted. The solution now takes the form

$$\begin{aligned} E_s &= C_{1s} \exp[ik_{sz}^m z + i\varphi_{1+}(z)] \\ &\quad + C_{2s} \exp[ik_{sz}^m z + i\varphi_{1-}(z)], \\ E_a^* &= C_{1a} \exp[-ik_{az}^m z + i\varphi_{1+}(z) - i(\Delta k)z] \\ &\quad + C_{2a} \exp[-ik_{az}^m z - i(\Delta k)z + i\varphi_{1-}(z)]. \end{aligned} \quad (62)$$

Here, φ_{1+} has a negative imaginary part which signifies gain. It is readily seen that $|E_s|$ and $|E_a|$ will first increase exponentially, and then level off as the laser power is depleted exponentially. We still have $|E_s|$, $|E_a|$, and $\varphi_1(z)$ as functions of Δk and $\Delta\omega$. The optimum intensity of $|E_a|$ occurs at some smaller value of Δk than that found in the last section.

The Stokes and anti-Stokes waves can of course act as sources in generating higher order Raman radiation as we shall now discuss.

VII. HIGHER ORDER RAMAN RADIATION

Raman radiation of many orders can be coupled together with the laser field through the nonlinear coupling connected by the fourth-rank susceptibility tensors. The latter can of course be derived either macroscopically as in Sec. II or microscopically as in Sec. III.

The problem of parametric generation of higher order Raman radiation is very complicated, because there are too many waves being coupled at the same time. If we

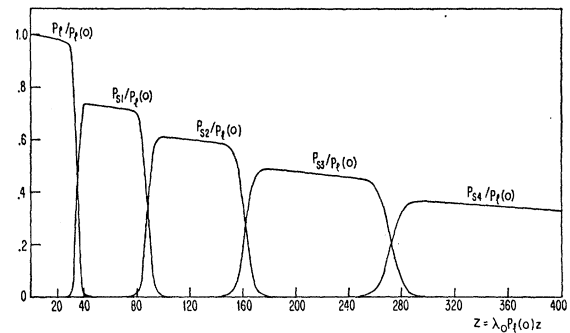


FIG. 10. The saturation effect of a single-mode laser beam of infinite extent. The intensities of the various orders of Stokes waves are normalized by the incoming laser intensity. The distance is also normalized to a dimensionless one $Z = \lambda_0 P_l(0) z$.

assume that the laser field has a single mode and uniform intensity distribution over large cross section, the problem is somewhat simplified in principle. As the example in Fig. 10 shows, the nonlinear nature of the problem is that two waves can be tightly coupled with high rate of energy transfer between them only when both have appreciable intensities. Moreover, the overlapping regions of tight coupling are rather narrow. The first approximation is therefore to regard these curves in Fig. 10 as square blocks, e.g.,

$$E_{sn} = E_{sn}^0 \quad \text{for } z_n \leq z \leq z_{n+1} \\ = 0 \quad \text{otherwise.}$$

This simplification suggests that we can solve the problem in steps.

First, waves at ω_s and ω_a are generated to saturation with the laser power completely depleted. Then, the ω_s and ω_a waves appear as sources to generate the second-order Raman radiation ω_{s2} and ω_{a2} , and the ω_l wave in the scattered direction. The latter process is described by the set of wave equations

$$\begin{aligned} \nabla^2 \mathbf{E}_{s2} + (\epsilon_{s2} \omega_{s2}^2 / c^2) \mathbf{E}_{s2} \\ = - (4\pi \omega_{s2}^2 / c^2) \{ \chi_1 \mathbf{E}_l^* \mathbf{E}_s \mathbf{E}_s + \chi_2 E_s \mathbf{E}_l \mathbf{E}_a^* \\ + \chi_3 (\sum_{k_s} \mathbf{E}_s) (\sum_{k_s} \mathbf{E}_s^*) \mathbf{E}_{s2} + \chi_4 \mathbf{E}_s \mathbf{E}_a \mathbf{E}_{a2}^* \}, \\ \nabla^2 \mathbf{E}_{a2} + (\epsilon_{a2} \omega_{a2}^2 / c^2) \mathbf{E}_{a2} \\ = - (4\pi \omega_{a2}^2 / c^2) \{ \chi_5 \mathbf{E}_a^* \mathbf{E}_l^* \mathbf{E}_s + \chi_6 \mathbf{E}_l \mathbf{E}_a^* \mathbf{E}_a^* \\ + \chi_7 \mathbf{E}_a^* \mathbf{E}_s^* \mathbf{E}_{a2} + \chi_8 (\sum_{k_a} \mathbf{E}_a) (\sum_{k_a} \mathbf{E}_a^*) \mathbf{E}_{a2}^* \} \quad (63) \end{aligned}$$

and similar equations for \mathbf{E}_l 's. The linear momentum matching conditions for the various terms are

$$\begin{aligned} \mathbf{k}_l^0 + \mathbf{k}_{s2}^0 &= \mathbf{k}_s^0 + \mathbf{k}_s^{0'}, \\ \mathbf{k}_a^0 + \mathbf{k}_{s2}^0 &= \mathbf{k}_s^0 + \mathbf{k}_l^0, \\ \mathbf{k}_s^0 + \mathbf{k}_{s2}^0 &= \mathbf{k}_s^{0'} + \mathbf{k}_{s2}^{0'}, \\ \mathbf{k}_{a2}^0 + \mathbf{k}_{s2}^0 &= \mathbf{k}_s^0 + \mathbf{k}_a^0, \\ \mathbf{k}_s^0 + \mathbf{k}_{a2}^0 &= \mathbf{k}_a^0 + \mathbf{k}_l^0, \\ \mathbf{k}_l^0 + \mathbf{k}_{a2}^0 &= \mathbf{k}_a^0 + \mathbf{k}_a^{0'}, \\ \mathbf{k}_a^0 + \mathbf{k}_{a2}^0 &= \mathbf{k}_a^{0'} + \mathbf{k}_{a2}^{0'}. \end{aligned} \quad (64)$$

As shown in Secs. IV and V, the nonlinear coupling terms will change the wave vector \mathbf{k}^0 to \mathbf{k} , and the maximum gain may occur in a direction slightly deviated from the linear phase-matched direction. With E_s and E_a highly directional, many sharp rings of E_{s2} and E_{a2} will be created.

In real experiments, the laser beam may contain many modes, and not all the laser power is depleted. Equation (63) will then describe the parametric generation of E_{s2} and E_{a2} through the interaction of the waves at ω_l , ω_s , and ω_a . The laser beam is in the forward direction. The first-order Stokes wave is emitted in a rela-

tively narrow aperture around the forward-backward direction, since there the interaction length for amplification is maximum for a laser beam with a cross section smaller than the cell length. The first-order anti-Stokes wave is generated near the phase-matched direction as we discussed earlier. If $|E_a| \ll |E_s| \ll |E_l|$, then to the first-order approximation the χ_4 , χ_7 , and χ_8 terms in Eq. (63) can be neglected. The χ_3 term is responsible for the forward-backward peaks in the second-order Stokes intensity. The χ_1 and χ_6 terms could only be phase matched for a direction of E_l off axis. These processes are clearly not likely to occur, since no initial laser pump intensity is available off axis. No E_l rings have ever been observed. The χ_1 term can also be phase matched by E_l in the forward direction and E_s in the off-axis directions. This would give rise to a diffuse, broad ring of E_{s2} and would be hard to detect experimentally. Thus, the conclusion of Terhune⁸ and Garmire, Pardarese, and Townes¹⁶ is confirmed that the observed E_{s2} and E_{a2} rings arise from the χ_2 and χ_5 terms, respectively.

When Raman components of many orders are simultaneously present with appreciable intensities, the situation becomes very complicated, since all waves are tightly coupled together. While approximation methods may be used to discuss the problem qualitatively, the rigorous and quantitative solution can only be obtained by solving the complete set of coupled wave equations.

VIII. MULTIMODE STRUCTURE AND FLUCTUATION PHENOMENA

Nonlinear phenomena should be described in a stochastic sense, as the incident laser field is usually composed of many modes, whose amplitude and phases are random variables. They are not necessarily statistically independent. The nonlinear processes in the laser medium may couple different modes and may establish partial or complete correlation between them. For a ruby laser, where different modes make use predominantly of different excited ions, the complex amplitudes can be considered as statistically independent. Ducuing and Bloembergen³⁹ have considered the multimode and fluctuation effect in the second harmonic generation.

In the case of Raman effect, the problem is much more complicated. Each individual laser mode generates a corresponding mode of Raman radiation. The many Raman modes are also coupled together through the Raman processes. As a result, the number of waves involved in the coupling scheme is greatly increased.

Let us consider as an example the generation of pure Stokes waves by a multimode laser beam. The highly damped vibrational wave with wave vector k_v has the form

$$\mathbf{Q}_v^*(\mathbf{k}_v) = (-\lambda/2\omega_v D^*) \sum_{n,n'} \mathbf{E}_{nl}^*(\mathbf{k}_{nl}) \mathbf{E}_{n's}(\mathbf{k}_{n's}), \quad (65)$$

³⁹ J. Ducuing and N. Bloembergen, Phys. Rev. 133, A1493 (1964).

where $\mathbf{k}_{n's} + \mathbf{k}_{n''} = \mathbf{k}_{n'l}$. The corresponding set of coupled wave equations for n modes of laser and Stokes waves is, neglecting dispersion,

$$\begin{aligned} \nabla^2 \mathbf{E}_{n's}(\mathbf{k}_{n's}) + (\omega_s^2 \epsilon_s / c^2) \mathbf{E}_{n's}(\mathbf{k}_{n's}) \\ = -4(\pi \omega_s^2 / c^2) \chi_s \sum_{n', n'', n'''} \mathbf{E}_{n'l}^*(\mathbf{k}_{n'l}) \\ \times \mathbf{E}_{n''s}(\mathbf{k}_{n''s}) \mathbf{E}_{n''l}(\mathbf{k}_{n''l}), \quad (66) \end{aligned}$$

$$\begin{aligned} \nabla^2 \mathbf{E}_{n'l}(\mathbf{k}_{n'l}) + (\omega_l^2 \epsilon_l / c^2) \mathbf{E}_{n'l}(\mathbf{k}_{n'l}) \\ = -(4\pi \omega_l^2 / c^2) \chi_s^* \sum_{n, n'', n'''} \mathbf{E}_{n''l}(\mathbf{k}_{n''l}) \\ \times \mathbf{E}_{n's}^*(\mathbf{k}_{n's}) \mathbf{E}_{n''s}(\mathbf{k}_{n''s}), \end{aligned}$$

where $\mathbf{k}_{n's} = \mathbf{k}_{n''l} + \mathbf{k}_{n''s} - \mathbf{k}_{n'l}$. For a large number of n , the solution of Eq. (66) is quite difficult. We can however, from direct inspection of the equations, derive the following general conclusions.

(1) If E_{nl} 's can be taken as constants, the solution of $E_{n's}$ will have the form

$$\mathbf{E}_{n's} = \sum_m A_{nm} \exp[i(\mathbf{k}_{nm}' + i\mathbf{k}_{nm}'')_s \cdot \mathbf{r} - i\omega_s t]. \quad (67)$$

(2) The amplitudes $|E_{n's}|$ will have the same rate of increase with distance, if all laser modes are of nearly the same intensity. If some laser modes, say E_{ml} , are much more intense, then the corresponding Stokes modes $E_{m's}$ will have much higher rate of increase in intensity than the others and get saturated much earlier. The Stokes modes corresponding to small E_{nl} may have their intensities increase at a rate predominantly determined by the nonlinear coupling terms $E_{nl} E_{ml}^* E_{m's}$ in the equations for $E_{n's}$.

(3) The detector to detect the Stokes waves will see a signal proportional to³⁹

$$\frac{1}{T} \int_0^T |\sum_n E_{n's}|^2 dt,$$

T being the characteristic time of the detector. It is, however, hard to estimate the fluctuations in the signal, since both A_{nm} and \mathbf{k}_{nm} in Eq. (67) depend strongly on the randomness of E_{nl} 's.

(4) The generation and amplification of the Stokes waves will deplete the power in laser modes. The laser mode with the strongest intensity will usually be depleted first.

(5) When the power in stronger laser modes is depleted, Eqs. (66) no longer represent the true situation. The Stokes wave in one mode will interact strongly with the laser wave in other modes to generate higher order Raman radiation. This higher order Raman radiation will then join the group of coupled waves. More generally, the presence of anti-Stokes waves of many modes will complicate the problem even more.

(6) Because of the nature of exponential gain, weak

modes have far less amplification than the strong ones. The Raman radiation would apparently have fewer modes.

IX. COMPARISON WITH EXPERIMENTS

The experiments reported so far were far from the ideal situation. The ruby laser beams were focused, non-uniform in intensity distribution, and of multimode structure. Moreover, the characteristics of the beams vary from shot to shot. It is therefore difficult to compare quantitatively the theoretical results with the experimental findings except for some special cases.

The resonant Raman susceptibility is given in Eq. (23). As a typical example, $\Gamma = 4.75 \times 10^{11} \text{ sec}^{-1}$ (corresponding to a half Raman linewidth of 2.5 cm^{-1}), $N = 10^{22} \text{ cm}^{-3}$, $\alpha_l = 10^{-23} \text{ esu}$, and $\eta = 1/5$, we find $\chi_R'' = 8 \times 10^{-13} \text{ esu}$. For a dense medium with a refractive index of $n = 1.58$, a Lorentz factor²² $L_c = (n_l^2 + 2)^2 \times (n_s^2 + 2)^2 / 81 \simeq 5$ should be applied to χ_R'' which then becomes $4 \times 10^{-12} \text{ esu}$. McClung and Weiner⁴⁰ measured the Raman scattering cross section for the 992 cm^{-1} benzene liquid line and found $(\eta^2 \alpha_l^2 / 100) L_c = (2.1 \pm 0.5) \times 10^{-49} \text{ cm}^6$, the Lorentz factor L_c being 4.92.³⁴ For a half linewidth of 2.5 cm^{-1} , one would find a Raman susceptibility $\chi_R'' = 4.2 \times 10^{-12} \text{ esu}$.

The nonresonant part of the Raman susceptibility is about an order of magnitude smaller than the resonant part. Maker *et al.*³⁰ measured intensity-dependent indices of refraction at the ruby frequency in many liquids. These are related to the fourth-rank susceptibility tensor $\chi(\omega = \omega + \omega - \omega)$, which should be of the same order of magnitude as the nonresonant Raman susceptibility. The values range from $8 \times 10^{-15} \text{ esu}$ for water to 10^{-12} esu for carbon disulfide with our amplitude convention. Terhune³⁴ also measured the Stokes susceptibility as a function of frequency in an organic liquid by irradiating it with radiation from a Raman laser, filled with different liquids with different vibrational frequencies near the vibrational frequency of the sample. He was able to reproduce a resonant curve for χ_s'' of the type shown in Fig. 2.

The power gain per cm of pure Stokes generation is given by

$$g_s = 4\pi \omega_s \chi_R'' |E_l|^2 / cn. \quad (68)$$

For the previous example with a laser power of 100 MW/cm^2 corresponding to $|E_l| = 320 \text{ esu}$, we find $g_s = 0.27 \text{ cm}^{-1}$. Hellwarth *et al.*⁴¹ estimated a power gain of 0.3 cm^{-1} for nitrobenzene at a pump level of 100 MW/cm^2 .

The dispersion for the optical phonon waves in the materials, where the stimulated Raman effect has been observed, is very small. The difference in frequencies of the forward and backward Stokes waves is certainly less

⁴⁰ F. J. McClung and R. Weiner (to be published).

⁴¹ R. W. Hellwarth, F. J. McClung, W. G. Wagner, and R. Weiner, *Bull. Am. Phys. Soc.* **9**, 490 (1964).

than the linewidth. We have $\beta(k_{vz}^0)_b^2 \lesssim 2\omega_v \Gamma$, and the expansion of Eq. (41) is justified. The second-order term in the equation is at least a factor $g_s/(k_{vz}^0)_b$ smaller than the first-order term, and can be neglected. It therefore cannot account for the forward-backward asymmetry in the Stokes generation. This asymmetry may be explained by the k_v dependence in the damping constant Γ . Stoicheff²⁰ found a forward-backward intensity ratio of 10:1. Terhune³⁴ observed a ratio 2:1 in his measurements on benzene. A difference of 5% in Γ for the two directions is enough to account for the effect, assuming a forward gain of e^{20} .

Apart from the dip near the phase-matched direction with the anti-Stokes radiation, the Stokes gain would be isotropic if the directional dependence of Γ is neglected. It is indeed possible to construct a Raman laser at an off-angle.⁴² Using a cylindrical lens to focus a laser beam, Dennis and Tannenwald⁴³ have achieved Stokes oscillation in a cavity at right angles to the laser beam.

The Stokes oscillation in a cavity starts when the Barkhausen condition Eq. (44) is satisfied. Assume $g_s = 2.7 \times 10^{-3} \text{ cm}^{-1}$ corresponding to a laser flux of 1 MW/cm². Then, for a 10-cm Raman cell, the reflectivity of the mirrors must be larger than 97.5% to ensure oscillation. At high-power levels, e.g., an amplification of e^{20} in a single traversal across the cell, a feedback of one part per billion will be sufficient to start the oscillation. The Raman laser action will deplete the laser power and build up the Stokes intensity to saturation.

The angular distribution of the first-order anti-Stokes intensity can be explained by the results of coupling-wave analysis in Sec V. In any direction, the coupled waves have some partial anti-Stokes character, which is given by Eq. (59). In the forward direction, $\Delta k \approx 10^2 \text{ cm}^{-1}$, the partial character $|E_a/E_s|^2$ would be 0.01% for a power gain of 2 cm⁻¹ in nitrobenzene. Because of the high intensity of the Stokes wave in the forward direction, the corresponding anti-Stokes radiation is strong enough to be detected. This has indeed been observed by many workers.⁴⁴

Near the linear phase-matched direction, the gain constant decreases (Fig. 8), but the partial anti-Stokes character increases. Figure 7 shows that the anti-Stokes intensity has an optimum for a momentum mismatch $\Delta k \approx 2g_s$. Consequently, there is a bright anti-Stokes ring appearing at an angle very close to but slightly larger than that of the exact phase-matched direction. This has been observed by Terhune and others.⁸⁻¹⁰ Chiao and Stoicheff¹⁰ have also reported a dark Stokes emission ring near the phase-matched direction in calcite. This is easily explained by the dip in the Stokes gain as shown in Fig. 9.

The angular deviation of the anti-Stokes ring from the linear phase-matched direction can be found from the relations in Eq. (52), corresponding to $\Delta k_x = (k_{sx} - k_{sx}^0)$ in the transverse momentum. We then find $\Delta\theta/\theta_0 = \Delta k_{sx}/k_{sx}^0 = \Delta k/2k_s^0 \tan^2 \theta_0$. If the direction of maximum anti-Stokes intensity occurs at $\Delta k = 2g_s$ for $g_s = 3 \text{ cm}^{-1}$ and $\theta_0 = 2.5^\circ$, we get $(\Delta\theta)_{\max} \approx 0.03^\circ$. It shows that to obtain good results, careful experimental arrangements should be used.

Chiao and Stoicheff¹⁰ have observed in calcite that the experimental direction is very close to the direction of momentum matching. The result is compatible with our theory. Many other workers have reported different angular patterns with deviation of 0.5° or more from the phase-matched direction. It appears that the angular pattern, as well as spectral distribution discussed above is very sensitive to the distribution of the laser power over various modes. Only very careful experimental arrangements which approximate single mode operation, could be used to test the theory in its present form.

For gases, the phase-matched direction is essentially the forward direction $k_{sx}^0 = 0$. The optimum anti-Stokes intensity occurs at an angle $\theta_{\max} \approx \Delta k_x/k_s^0 \approx (\Delta k/k_s^0)^{1/2}$. For $g_s = 4 \text{ cm}^{-1}$, and $\Delta k = 2g_s = 8 \text{ cm}^{-1}$, the angle is 10^{-2} rad or 0.57° . The Stokes intensity should also have a dip in the forward direction. This is presumably obscured by scattering and by geometrical factors.

The saturation effect in the stimulated Raman radiation is commonly observed.^{34,35,45} If the laser flux density is 1000 mW/cm², then, in a single traversal across a 15-cm nitrobenzene cell, the Stokes gain would be e^{45} . This means that a single photon would have created 10^{20} photons. This number is however larger than the initial number of laser quanta in the pulse, which is less than 10^{18} . The laser beam is exhausted before it reaches the end of the cell. Usually, a gain of 10^{10} will start the saturation. The first-order Raman radiation can build up to serve as the pump for the second-order Raman radiation, and so on. The output power will spill over into more and more Raman components of comparable intensities as the laser power is increased.⁴⁵ Terhune³⁴ has reported measurements on the intensities of Raman radiation of many orders. In the real experiments, the laser power is never completely exhausted, because there are always parts of the cross section with relatively low intensities. The power in these areas, which may often amount to more than 40%, is not converted. More than 60% of output power at Stokes frequencies has been observed in a Raman laser. This percentage should be higher, were it not for the fact that the laser beam is far from a homogeneous plane wave and has many modes. From the standpoint of conversion, a ruby laser with a few very bright filaments and a few very strong modes would be better than a homogeneous cross section of many modes with

⁴² H. Takuma and D. A. Jennings, Appl. Phys. Letters 4, 185 (1964).

⁴³ J. H. Dennis and P. E. Tannenwald, Appl. Phys. Letters 5, 58 (1964).

⁴⁴ G. H. Dieke and P. Lallemand (private communications).

⁴⁵ H. Takuma (private communications).

the same total power. The variation of intensity of the laser modes with time during the pulse is also important.

Higher order Stokes and anti-Stokes rings have been observed.⁸⁻¹⁰ Terhune⁸ and Garmire *et al.*¹⁶ have suggested that these rings are generated successively. The angular position is determined by the linear phase-matching condition. For the n th anti-Stokes ring $\mathbf{k}_l + \mathbf{k}_{an} = \mathbf{k}_a + \mathbf{k}_{a(n-1)}$ and for the n th Stokes ring, $\mathbf{k}_l + \mathbf{k}_{s(n-1)} = \mathbf{k}_a + \mathbf{k}_{sn}$. The comparison with experimental results is beset by the same difficulties and discrepancies as were mentioned for the first anti-Stokes case. As pointed out in Sec. VII, the rigorous solution of the problem should be obtained from the coupled-wave approach, and the angular positions of the rings may deviate slightly from the linear phase-matched direction. The coupled-wave solution may give broadened Raman spectra. Stoicheff²⁰ has reported peculiar broadening of the Stokes and anti-Stokes lines. Whenever the laser spectrum was composed of two lines 0.8 cm^{-1} apart, the Raman spectra were asymmetrically broadened to as much as 10 or 50 cm^{-1} . The broadened spectra consisted of a series of maxima and minima with a period of about 0.8 cm^{-1} . The fact that the Stokes and anti-Stokes waves are intense enough to couple and beat together many times with the laser wave components may well explain such a broadening effect. A detailed analysis has however not yet been made. Many other workers have observed broadened spectral distributions of the Stokes and anti-Stokes components. They do not state whether the spectral distribution in the laser pump is an important factor.

Experiments reported so far are not sufficiently well defined to provide a test of the theory, nor can they unravel the various physical mechanisms in the stimulated Raman effect. The behavior of a small signal amplifier rather than a high-level oscillator would be more informative. Therefore, very thin Raman cells, which are not capable of sustaining oscillation, should be used. A small signal at ω_s or ω_a but large compared to noise, is incident on the cell. The gain can be measured, and kept below 3 dB, so that depletion of laser power and creation of higher order Raman radiation can be neglected. Ideally, one would like to have a single-mode laser beam with uniform intensity over its cross section. One would also like to control intensities, polarizations, directions, and frequencies of the incident

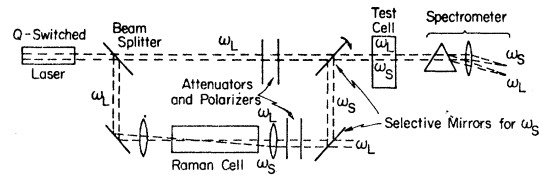


FIG. 11. Experimental arrangement for the measurement of Raman susceptibilities. The Stokes gain can be determined as a function of intensity, direction, and polarization of both laser and Stokes beams, in a short sample call.

laser and Stokes beams independently. Such experiments would then be capable of yielding reliable information on the characteristics of the Stokes and anti-Stokes amplification. The values of Raman susceptibilities could also be obtained. A possible experimental arrangement is shown in Fig. 11. A powerful laser beam passing through a mode selector is split, and one fraction of it generates Stokes radiation in a Raman cell. The laser light is filtered out. The Stokes radiation is, after suitable attenuation and polarization, recombined with the other part of the laser beam in a variable direction. The two beams then traverse the thin sample cell. The gain is measured as a function of direction, etc. The amplification of anti-Stokes radiation near the phase-matched direction can also be measured. Similar experiments have already been carried out by Terhune,³⁴ and by Bret and Mayer.³⁵ However, the laser beams used in their experiments consisted still of many modes, and the direction of laser and Stokes beams could not be controlled independently; results are therefore subject to large uncertainties.

X. CONCLUSION

A detailed account of the theory of stimulated Raman and Brillouin effects is given. They are described classically as the results of coupling between the light waves and the optical and acoustic vibrational waves. In this framework, many of the experimental observations can be explained at least qualitatively. However, the theory is based on drastic simplification of the problem, and therefore direct comparison of the theory with already performed experiments is not possible. The details of the theory can only be tested with further refinement of the experiments.